

DETERMINATION OF SHOT PEENING EFFECT ON FATIGUE BEHAVIOR
OF AISI 4140 STEEL BY NON-DESTRUCTIVE MEASUREMENT OF
SURFACE RESIDUAL STRESSES

A THESIS SUBMITTED TO
THE GRADUATE SCHOOL OF NATURAL AND APPLIED SCIENCES
OF
MIDDLE EAST TECHNICAL UNIVERSITY

BY

SALİM ÇALIŞKAN

IN PARTIAL FULFILLMENT OF THE REQUIREMENTS
FOR
THE DEGREE OF MASTER OF SCIENCE
IN
METALLURGICAL AND MATERIALS ENGINEERING

JANUARY 2018

Approval of the thesis:

**DETERMINATION OF SHOT PEENING EFFECT ON FATIGUE
BEHAVIOR OF AISI 4140 STEEL BY NON-DESTRUCTIVE
MEASUREMENT OF SURFACE RESIDUAL STRESSES**

submitted by **SALİM ÇALIŞKAN** in partial fulfillment of the requirements for the degree of **Master of Science in Metallurgical and Materials Engineering Department, Middle East Technical University** by,

Prof. Dr. Gülbin Dural Ünver
Dean, Graduate School of **Natural and Applied Sciences** _____

Prof. Dr. C. Hakan Gür
Head of Department, **Metallurgical and Materials Engineering** _____

Prof. Dr. C. Hakan Gür
Supervisor, **Metallurgical and Materials Eng. Dept., METU** _____

Examining Committee Members:

Prof. Dr. Tayfur Öztürk
Metallurgical and Materials Engineering Dept., METU _____

Prof. Dr. Rıza Gürbüz
Metallurgical and Materials Engineering Dept., METU _____

Prof. Dr. C. Hakan Gür
Metallurgical and Materials Engineering Dept., METU _____

Prof. Dr. Abbas Tamer Özdemir
Metallurgical and Materials Engineering Dept., Gazi University _____

Assist. Prof. Dr. Mert Efe
Metallurgical and Materials Engineering Dept., METU _____

Date: 25.01.2018

I hereby declare that all information in this document has been obtained and presented in accordance with academic rules and ethical conduct. I also declare that, as required by these rules and conduct, I have fully cited and referenced all material and results that are not original to this work.

Name, Last name: Salim ÇALIŞKAN

Signature :

ABSTRACT

DETERMINATION OF SHOT PEENING EFFECT ON FATIGUE BEHAVIOR OF AISI 4140 STEEL BY NON-DESTRUCTIVE MEASUREMENT OF SURFACE RESIDUAL STRESSES

Çalışkan, Salim

M.Sc., Department of Metallurgical and Materials Engineering

Supervisor: Prof. Dr. C. Hakan Gür

January 2018, 97 pages

The fatigue performance of aircraft parts can be improved by inducing compressive residual stresses in the near-surface zone by shot-peening. The depth profile and the magnitude of residual stresses depend on the shot peening parameters. Aircraft industry requires an easy and rapid non-destructive method for determination of residual stress state to verify the achievement of the desired results of shot-peening. This study aims to determine nondestructively the residual stresses at the surface by the Magnetic Barkhausen Noise (MBN) method, and also, to investigate the effect of the shot peening severity on the fatigue life of AISI 4140 steel. By this way, it might be possible to correlate the MBN measurement results with fatigue life and to verify nondestructively the success of shot-peening process to achieve the desired fatigue life.

Keywords: Steels, Shot-peening, Residual stress, Fatigue, Nondestructive evaluation, Magnetic Barkhausen Noise

ÖZ

BİLYELİ DÖVME İŞLEMİNİN AISI 4140 ÇELİĞİNİN YORULMA DAVRANIŞINA ETKİSİNİN YÜZEY KALINTI GERİLMELERİNİN TAHRİBATSIZ OLARAK ÖLÇÜLMESİYLE BELİRLENMESİ

Çalışkan, Salim

Yüksek Lisans, Metalurji ve Malzeme Mühendisliği Bölümü

Tez Yöneticisi: Prof. Dr. C. Hakan Gür

Ocak 2018, 97 sayfa

Uçak parçaların yorulma ömürleri, bilyeli dövme işlemiyle yüzeyine yakın bölgelerde basma nitelikli kalıntı gerilmeleri oluşturularak uzatılabilir. Kalıntı gerilmelerinin derinlik profili ve büyüklüğü bilyeli dövme işlem parametrelerine bağlıdır. Havacılık sektörü bilyeli dövme yöntemi uygulanmış parçalardaki kalıntı gerilimini ölçmek için hızlı ve kolay bir tahribatsız muayene yöntemine ihtiyaç duymaktadır.

Bu çalışma bilyeli dövme işleminin AISI 4140 çeliklerindeki yorulma ömrüne olan etkisini ve parça yüzeyinde oluşan kalıntı gerilmelerin Manyetik Barkhausen Gürültüsü yöntemiyle tahribatsız olarak belirlenerek incelemeyi amaçlamaktadır. Bu sayede, MBN ölçüm sonuçlarının yorulma ömrüyle ilişkilendirilmesi ve bilyeli dövme işleminin başarısının tahribatsız olarak doğrulanması mümkün olabilir.

Anahtar Kelimeler: Çelikler, Bilyeli dövme, Kalıntı gerilme, Yorulma, Tahribatsız değerlendirme, Manyetik Barkhausen Gürültüsü

To My Parent

ACKNOWLEDGEMENTS

The author wishes to express his deepest gratitude to his supervisor Prof. Dr. C. Hakan Gür for his guidance, advice, criticism, encouragements, insight throughout the research and opportunity to work under his supervision on this study.

The author would also like to thank Dr. İbrahim Çam for his valuable suggestions and comments during thesis period.

The author intends to deliver his thankfulness to Turkish Aerospace Industry (TAI) because of support and permission to perform tests in its premises.

The author would like to acknowledge Mrs. Zeren Özgeneci and ORS company for XRD measurements.

My special thanks reserve to Mr. Alp Aykut Kibar, Mr. Fazlı Fatih Melemez, Mr. Mesut Talha Güven and Mr. Mehmet Çağırıcı for their support throughout this research.

Finally, I would like to thank my parents to present me exceptional life and unrequited love.

TABLE OF CONTENTS

ABSTRACT	v
ÖZ	vi
ACKNOWLEDGEMENTS	viii
TABLE OF CONTENTS	ix
LIST OF TABLES	xi
LIST OF FIGURES	xii
CHAPTERS	
1. INTRODUCTION.....	1
1.1.MOTIVATION	2
1.2.AIM OF THE WORK AND MAIN CONTRIBUTION.....	3
2. BASIC KNOWLEDGE	5
2.1.RESIDUAL STRESS.....	5
2.2.SHOT PEENING	7
2.2.1.SHOT PEENING PARAMETERS.....	10
2.2.1.1.SHOT INTENSITY	10
2.2.1.2.SHOT COVERAGE	12
2.2.1.3.SHOT MEDIA	13
2.2.2.INSTABILITY IN SHOT PEENING	14
2.2.3.PLASTIC DEFORMATION CAUSED BY SHOT PEENING	16
2.2.4.INFLUENCE OF SHOT PEENING ON FATIGUE LIFE.....	18
2.2.5.OPTIMIZATION OF PEENING PARAMETERS TO EXTEND THE SERVICE LIFE.....	22
2.2.6.SHOT PEENING OVERVIEW	25
2.3.EFFECT OF RESIDUAL STRESSES ON FATIGUE LIFE	26
2.4.MAGNETIC BARKHAUSEN NOISE METHOD	28

2.4.1.MBN DEPTH EVALUATION.....	36
2.4.2.MAGNETIC BARKHAUSEN NOISE SYSTEM.....	38
2.4.3.MBN OPERATION METHOD	39
2.4.4.ACCURACY IN MBN SYSTEM	41
2.5.DETERMINATION OF RESIDUAL STRESS BY MBN TECHNIQUE	43
2.6.RESIDUAL STRESS ANALYSIS BY X-RAY DIFFRACTION	45
2.6.1.BASICS OF XRD RESIDUAL STRESS EVALUATION	48
2.6.2.RESIDUAL STRESS MEASUREMENT TECHNIQUE	50
2.6.3.SOURCES OF UNCERTAINTIES	53
3. LITERATURE REVIEW	55
4. EXPERIMENTAL PROCEDURE	61
4.1.MATERIAL.....	61
4.2.SAMPLE PREPARATION	61
4.3.SHOT PEENING PARAMETERS.....	62
4.4.SURFACE ROUGHNESS MEASUREMENT	64
4.5.RESONANT FATIGUE TESTING	66
4.6.MAGNETIC BARKHAUSEN NOISE MEASUREMENT	67
4.7.CALIBRATION	68
5. RESULTS AND DISCUSSIONS.....	75
5.1.MICROSTRUCTURE OF THE SAMPLE	75
5.2.RESULTS OF MAGNETIC BARKHAUSEN NOISE MEASUREMENT.....	75
5.3.RESULTS OF XRD MEASUREMENTS	83
5.4.RESULTS OF FATIGUE TESTS	84
6. CONCLUSIONS.....	91
REFERENCES	93

LIST OF TABLES

TABLES

Table 1 Machining parameters of the AISI 4140 steel samples.....	61
Table 2 Almen Strip Results	64
Table 3 Surface roughness parameter values	65
Table 4 Frequency ranges and corresponding skin depth values	74
Table 5 MBN μ scan results.....	82
Table 6 XRD measurement results	83
Table 7 Fatigue test result for each parameter	86

LIST OF FIGURES

FIGURES

Figure 1 Residual stress versus skin depth [28].....	6
Figure 2 Representative shot peening operation [24]	8
Figure 3 Shot peened turbine blades [25]	9
Figure 4 Almen Strip Measurement Procedure [26].....	11
Figure 5 Partial (left) & full (right) coverage cases [27]	12
Figure 6 Examples of different shot media [27]	13
Figure 7 Typical residual stress distribution in the cross-section of the shot-peened material [27].....	17
Figure 8 Micro crack formation on the surface: unpeened (left) and shot peened (right) [29].....	19
Figure 9 Improvement of endurance limit via shot peening [30]	21
Figure 10 Properly shot peened (left) versus over peened (right) [31].....	22
Figure 11 Improvement of crack closure by shot peening [32]	24
Figure 12 Enhancement of fatigue life via polishing [33]	28
Figure 13 Magnetic hysteresis curve [21].....	30
Figure 14 Magnetic hysteresis loop and Barkhausen jumps [19].....	32
Figure 15 Representative magnetic domain: Unmagnetized (Left) and magnetized (Right) [20]	33
Figure 16 Orientation of domain wall with respect to applied stress: $\sigma < 0$ (middle), $\sigma = 0$ (left) and $\sigma > 0$ (right) [4]	36
Figure 17 Schematic MBN system: (a) electromagnetic yoke; (b) specimen; (c) coil [23]	37
Figure 18 Observation of Magnetic Barkhausen Noise [38]	40
Figure 19 Variation of MBN voltage pulses with stress [22]	44
Figure 20 Given two orientations: $\psi = 0$ (left) and rotation ψ angle (right) [34]	47
Figure 21 Constructive interference of reflected waves [35].....	48
Figure 22 A typical spectrum of emitted X-Rays from an X-Ray tube [35]	52
Figure 23 Depth profile of residual stress in shot-peened AISI 4140 steel [16].....	56
Figure 24 Stair case method to determine fatigue life [2]	57
Figure 25 Effect of surface roughness on fatigue life [17]	58

Figure 26 Effect of shot media parameter on the magnitude of compressive residual stress [1]	59
Figure 27 Drawing of the fatigue test specimen [37].....	62
Figure 28 Shot peening equipment (TAI)	62
Figure 29 Deflection of Almen strip	64
Figure 30 Scatter of surface roughness	66
Figure 31 Rumul resonant fatigue machine (TAI M&P Lab.).....	66
Figure 32 Stresstech MBN System (METU Central Lab.)	67
Figure 33 Scatter of MBN parameter (Roll-Scan Measurements).....	69
Figure 34 Calibration curve (initial sample)	70
Figure 35 Nanovolt, Micro Ohm Meter (METU Central Lab.)	71
Figure 36 Precision Impedance Analyzer (METU Central Lab.)	72
Figure 37 Diagram of a circular cross sectional toroid inductor [36].....	73
Figure 38 Change of the skin depth with frequency	74
Figure 39 Representative micrograph of the samples	75
Figure 40 Variation of MBN r.m.s. value with the severity of shot peening.....	76
Figure 41 Variation of surface residual stress with shot-peening parameters (determined from MBN measurements).....	77
Figure 42 Variation of surface residual stress with Almen intensity (%200 coverage)..	78
Figure 43 Variation of surface residual stress with Almen intensity (%300 coverage)..	78
Figure 44 Variation of surface residual stress with coverage (3A-6A intensity).....	79
Figure 45 Variation of surface residual stress with coverage (4A-7A intensity).....	79
Figure 46 Variation of surface residual stress with coverage (6A-10A intensity).....	80
Figure 47 Representative hysteresis curves for different shot peening intensities	81
Figure 48 Representative hysteresis curves for different shot coverage values.....	81
Figure 49 MBN profile versus magnetic field strength plot	83
Figure 50 Fatigue test results at 700 MPa maximum stress.....	85
Figure 51 Fatigue test results for 750 MPa maximum stress (3 sets for each sample type)	86
Figure 52 Effect of residual stress on fatigue life under maximum stress at 750 MPa (MBN measurement).....	87
Figure 53 Representative fracture surfaces for each sample group	88
Figure 54 Representative SEM micrograph showing cleavage and ductile regions	89
Figure 55 Fracture surfaces: SP3 [3A-6A %200] (left) & SP24 [6A-10A %300] (right)	89

CHAPTER 1

INTRODUCTION

Shot peening operation is exerted to machined components to form compressive residual stress on their surface layers; eventually, it will upgrade material properties. In other words, formed compressive residual stresses on the surface of material enhance fatigue strength of component, prevent fretting fatigue, and suppress stress-corrosion under operation. To acquire high quality shot peening operation, optimum compressive residual stress shall be introduced on the surface and subsurface of the component. Hereby, selection of optimum parameters is critical to make sure having ideal variations of residual stresses in the layer of work hardening so that the desired properties can be obtained. At first glance, determination of formed residual stress is mostly qualified by many nondestructive techniques as well as destructive testing methods implemented to samples. In case of continuous production of machine components, measurements at a sufficiently large number of them are required to be accomplished, and the compatibility of operation to be endorsed by statistical analysis of the outputs acquired.

Non-destructive techniques have currently become enounced, exclusively because of their feasibility to material analyses of components and their relevance for integration into automated production systems. Companies having automated production system employ on-line monitoring of the status of processing components, assured by many non-destructive techniques. The advantage of non-destructive technique is adequately reliable, fast, and reproducible. For well-done integration of the complicated non-destructive

testing techniques, the progress of sensor for collecting signals and data logger for processing and evaluation of test results become inevitable.

Among non-destructive techniques, Magnetic Barkhausen Noise allows micro-magnetic investigation for ferromagnetic materials. In other words, this technique enables to analyze microstructure and micro hardness of a material non-destructively and provides establishment of the extent and variation of formed residual stresses on the surface of component. The technique attached to MBN signals is derived from the present fact for any ferromagnetic materials on which it is magnetized by the alternating current. Microstructure encloses tiny magnetic zones which is called magnetic domains. Upon a ferromagnetic material is exposed to magnetic field, a flow of magnetic-domain walls takes place; herein, size and shape of domain walls are affected due to change in microstructure. Voltage jumps are caused by any abrupt increase in the magnetic flux; MBN signal is collected by appropriate sensor to attain data analysis.

Premature fatigue failure occurs abruptly and leads to severe damage. Fatigue damage and tolerance knowledge are critical in the design stage of operated systems. Therefore, presuming the life of the component depending on alternating stress is inevitable not to encounter with catastrophic failure. As a result, SN curves were introduced to estimate endurance of component under cyclic loading. To represent ideal case of operation, coupon level of testing is required to predict life of component under constant load amplitude. Then, behavior of the component can be correlated based on acquired data.

1.1. MOTIVATION

Fatigue behavior is very critical to determine limits of materials in aviation field. Fatigue failures often occur quite suddenly with disastrous results and fatigue is most unreliable for metals. Fatigue causes brittle like failures even in normally ductile materials with little gross plastic deformation occurring prior to fracture. The process occurs by the initiation and propagation of cracks and, ordinarily, the fracture surface is so close to perpendicular direction of maximum tensile stress.

The fatigue life of aircraft parts can be improved by shot peening. The typical application examples are landing gears, various gearbox components, drive and crank shafts and turbine components. Shot-peening creates compressive residual stresses on the surface of the component depending on the various process parameters.

AISI 4140 is a low alloy steel containing chromium and molybdenum and exhibits good overall combinations of strength, toughness, wear resistance and fatigue strength. In addition, it is a versatile alloy with good atmospheric corrosion resistance and reasonable strength up to around 315° C. It is frequently used in aircraft parts such as axles, conveyor parts, crow bars, gears, logging parts, spindles, shafts, pump shafts, sprockets, studs, pinions, rams, and ring gears.

The aircraft industry requests an easy and rapid non-destructive method for determination of residual stresses to verify the successful results of shot-peening on the whole component.

1.2. AIM OF THE WORK AND MAIN CONTRIBUTION

The purpose of this study is to monitor the variation of surface residual stresses on the shot peened steels by Magnetic Barkhausen Noise measurement and to investigate the effect of shot peening parameters on residual stresses and fatigue life. In order to achieve this, AISI 4140 steel specimens were shot peened for different peening intensities and coverage percentages. Fatigue tests were carried out by resonant fatigue testing machine which allows very high test frequencies. Then, residual stress state versus fatigue life plot was constructed.

Shot peening severity affects the residual stress state on the surface and eventually fatigue life of the component. If surface residual stress state can be evaluated by Magnetic Barkhausen Noise method; then, it is possible to estimate fatigue life of the shot peened steels in a fast, practical and non-destructive way.

Surface residual stress caused by various shot peening parameters such as peening intensity and coverage percentage were measured by the MBN method and the optimum peening parameters to obtain the maximum compressive residual stresses on the surface of the AISI 4140 steel were determined. In addition, the effect of surface residual stresses created by shot peening on the fatigue life of the AISI 4140 steel was investigated. Critical data that are useful for the fatigue design of AISI 4140 steel components was obtained.

CHAPTER 2

BASIC KNOWLEDGE

2.1. RESIDUAL STRESS

Residual stresses are defined as existence of internal stresses on the workpiece after removal of external loads. Any material in service have more or less residual stress in a body and never show stress-free condition. Thus, residual stresses have significant influence on performance of material.

The formation mechanism of residual stresses is caused by many diverse event. Structural mismatching and non-uniform distribution of non-elastic strains such as thermal and plastic strains are common phenomenon behind of formation mechanism. Basically, applied production method, microstructure of material and exposed processing like wear are the main reasons for emergence of internal stresses. Residual stresses are formed between several grains, in a single grain or in a point depending on circumstances. Internal forces caused by residual stress are in an equilibrium across the affected region. In case of any external intervention, equilibrium can be impaired depending on type of residual stresses.

In the course of machining operation, generated residual stresses could be positive or negative and sign of internal stress is critical in terms of stress corrosion resistance and fatigue performance of material. Therefore, machining parameters like feed rate or cutting speed shall be optimized to attain maximum performance.

Shot peening or induction hardening causes formation of compressive residual stresses and those enhance fatigue life of material under alternating loading by preventing crack

formation. In shot peening case, magnitude of the residual stress varies with skin depth of the component and maximum value of the residual stress that is highest induced stress is determined by stress versus skin depth graph as shown in *Figure 1*. The residual stress magnitude can be measured up to half of the yield strength of the material during shot peening operation.

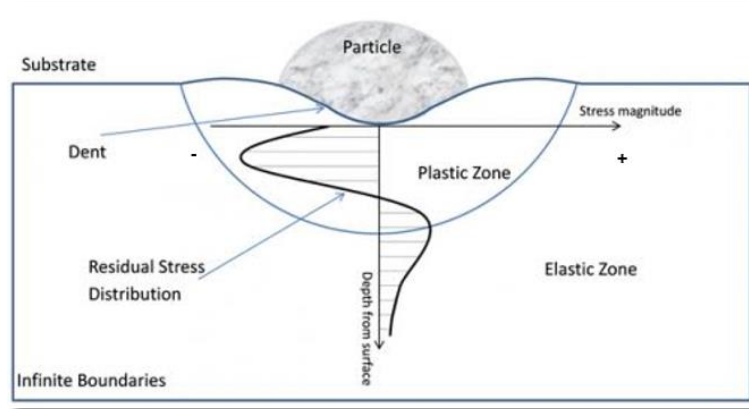


Figure 1 Residual stress versus skin depth [28]

The skin depth of the material depends on several shot peening parameters. Also, effect of those parameters alters depending on material characteristic. For instance; effect of shot intensity shows dissimilarity between 7050 T7451 alloy and 15-5 PH steel in terms of skin depth.

Surface hardening provides enhancement in fatigue life due to formed compressive residual stress on the surface of the material. Similarly, some surface finishing processes like honing, polishing enable to get rid of discontinuities on the surface that enhances the fatigue life of the material. Among them, most popular one is shot peening operation due to controlled of the process and homogeneity of stress distribution. As a cold working operation; shot peening is beneficial process since it retains compressive residual stress on the surface of component. It is well known that fatigue crack initiates on the surface of the material. Therefore, it severely enhances fatigue life of the material. Hereby, the

critical point is to choose optimum shot peening parameters to be able to achieve best process results.

Fatigue properties of the component are greatly affected by manufacturing processes like EDM, grinding, welding. Moreover, the fatigue life of component is severely impressed by surface roughness. For instance, EDM (Electro-Discharge Machining) operation may retain tensile residual stress on the surface of material by producing recast layer that is brittle and fatigue crack originates in this layer and later propagates inside the material; as a result, it causes detrimental effect on the fatigue life of component.

Grinding operation forms tensile residual stress on the surface of the component. It dramatically reduces the fatigue life of the component. Formed tensile residual stress by grinding is approximately close to ultimate tensile stress of the material. Detrimental effect on fatigue of the operation can be compensated by applying shot peening after grinding process.

2.2. SHOT PEENING

The shot peening process is basically cold working operation by addressing spherical shots on the surface of the material within a certain time. During operation, each striking shot behaves like a hammer by forming a small dimple on the surface of component. To be able to generate compressive stress on the surface of the component; surface part shall be reacted in tension. After hitting the shot media on the surface of the component; atoms just below the surface attempt to spring back their original position. As a result; this causes formation of dimples and compressive residual stress is formed on the surface of the material. During fatigue testing, cracks initiate and propagate on the surface of the material. Formed compressive stress because of shot peening causes increase in the life of component in terms of fatigue and stress corrosion failures. Thus, shot-peening is an effective way to prevent unexpected failure for cyclic loading conditions. Approximately half of the yield strength as being compressive stress on the surface could be achieved in the case of maximum shot peening parameters that provokes substantial amount of

increase in the fatigue life of the component. On the other hand, cold working operation results in decrease in the surface roughness of the component that inversely affects the life of the material. To conclude; shot peening severely enhances the fatigue failures, stress corrosion fatigue, stress, hydrogen assisted cracking, fretting, and erosion caused by cavitation. The cold working operation enables to improve intergranular corrosion resistance and surface texturing and assists to close of porosity.

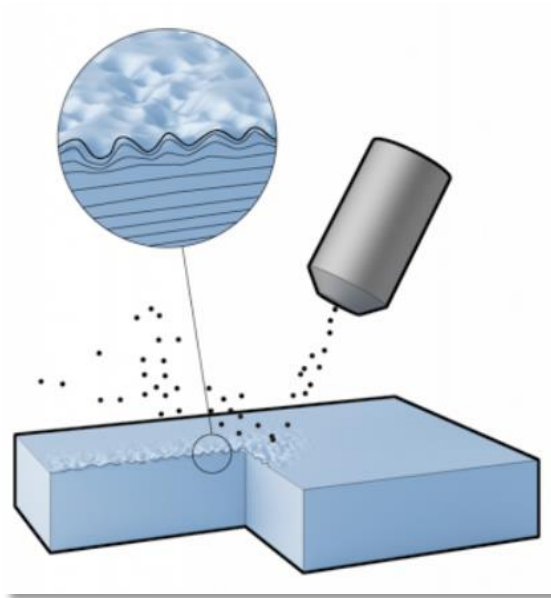


Figure 2 Representative shot peening operation [24]

Shot peening possesses minor or even no effect on structures such as buildings or bridges that are loaded statically. Its impact is observed well for cyclically loaded structures. Common applications for shot-peening can be exemplified as all the coil, leaf and valve springs as well as the torsion rods, drive shafts, axles, and gears in automobile industry. In addition, shot peening also lends to integrity of parts of aircraft in aerospace industry like aluminum and titanium as well as steel parts. Shot peened is applied to the wind sins and structural members to enhance their fatigue life as well as to avoid stress corrosion cracking. The landing gear is also shot peened and most parts in the jet engines as shown

in *Figure 3*. Railroad wheels, rotary printing press plates, aircraft propellers, high strength fasteners, rock drilling bits, and drill rods are other common shot peened parts.



Figure 3 Shot peened turbine blades [25]

It is well known that all the metals fail under tension loading not under compressive loading. The crack causing failure will generally initiate on the surface of the material where highest tension stresses is available and a stress riser exists like scratch, dent, machine mark, etc. that enables increasing stress concentration on the tip of the defect. Upon shot peened parts have been loaded cyclically; as a result, the failure resulted by tensile stresses is minimized by the amount of the compressive stresses retained due to shot peening operation. Shot peening enables decreasing affected tensile stress on the front of crack tip due formed compressive residual stress on the surface which means it needs to be applied higher stresses to propagate the crack and also increases service life of the component. When the skin depth of the induced compressive stress layer due to shot peening surmounts the depth of all surface defects aforementioned above; the initiation of crack is annihilated. This can be commented as the basic mechanism behind of the shot peening operation.

The compressive residual stress up to the half of the yield strength of the material can be obtained depending on the selected process parameters. Hereby, size and condition of the peening media, the time that material is exposed to the blast stream, the size and configuration of the nozzles, angles, distances and other related factors control exactly the depth of the compressed layer and the distribution of the residual stress. Eventually, improved service life of the component can be achieved. To optimize the shot peening parameters is vital especially in aerospace industry. The control of the parameters is critical since consistency of one component to another meet same quality. It shall be ensured that alternative measurement technique like Almen gage measurement for consistency of intensity of shot peening.

2.2.1. SHOT PEENING PARAMETERS

2.2.1.1. SHOT INTENSITY

Many parameters like shot size, type of material used as the spherical shot, the velocity of particles leaving blast nozzle and angle that particles screening across the surface are critical to obtain optimized shot peening process. Shot intensity is defined as ability to control the energy of the shot stream by changing the media size and shot velocity. Because of difficulties to measure peening intensity of each component; easy and simpler way is performed to quantify the intensity. A simple flat strip which is called as Almen strip is also shot peened on the side of the component as shown in *Figure 4*. After shot peening operation, flat strip becomes convex geometry that helps to measure intensity of the component. Hereby, the critical point is to determine the degree of curvature of the Almen strip. The curvature becomes higher at higher intensity applications.

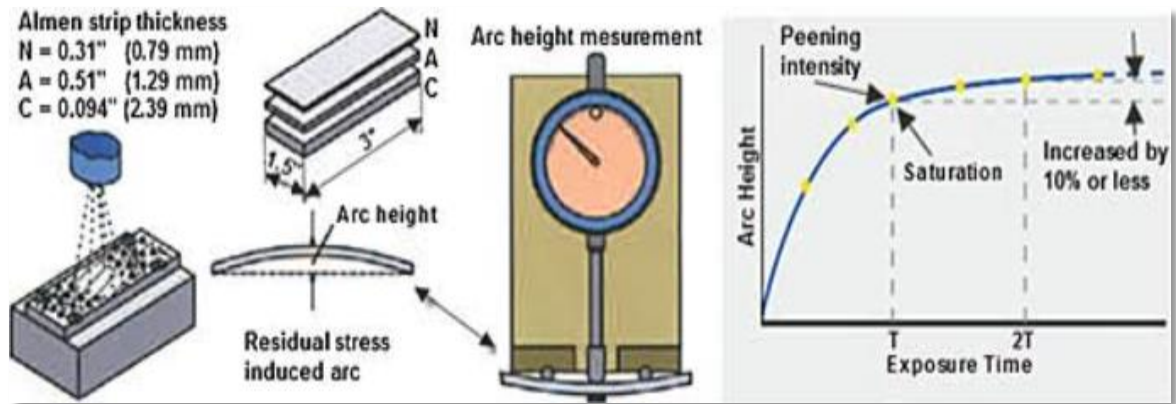


Figure 4 Almen Strip Measurement Procedure [26]

The standard Almen Strip is manufactured from spring steel in controlled dimensioning. Three Almen thicknesses exist and they called as C, A and N strip. Herein, C strip is the thickest one and N strip is the thinnest one. The curvature of the strip after process is measured by the help of Almen gauge. Strip is settled and retained magnetically against two pairs of ball that contacts a fixed distance apart. The gauge is balanced according to the initial strip position. Shot peened strip is settled against the contacts with the unpeened side towards the dial gauge stem; as a result, the Almen strip height is measured immediately in thousandths of an inch or millimeters. To ensure measuring diverse shot peening intensity, three Almen thicknesses are used. The most popular one is A strip among others. Generally, most shot intensity is chosen between 0.012 in A and 0.020 in A. If the intensity is less than 0.006 in A, the N type strip whose thickness is three times of A strip is used; on the other hand, C type is used in the case that intensity is higher than 0.23 in A. Almen intensity values is represented either inch or mm unit. For instance; 0.1 mm Almen intensity is also signified as $10A^2$ Almen intensity. In order to convert these values to the SAE standard; it shall be multiplied by 40. As a result; 0,1 mm Almen intensity corresponds to 4A and other measurements are performed according to this approach.

To quantify the shot intensity; Almen strip is needed and presents effective way because of its simplicity. The critical point is to assure one side of the Almen strip shall be exactly

same blast condition with peened one. To perform this, Almen strip is clamped by Almen block that is hardened steel. Then, the component and Almen strip are peened through shot stream. More than one strip is required for irregular geometries.

The time of exposure is critical to obtain intended Almen intensity besides shot size, velocity of shot nozzle, pressure etc. It is well known that intensity rises by holding longer time of shot blast stream. However, holding longer times does not mean that shot intensity increases linearly. It increases until saturation point then starts to decrease; nevertheless, saturation point can be compensated by increasing shot size which means higher intensities can be obtained higher shot size. Generally, optimized shot intensities in the specifications state materials saturation values.

2.2.1.2. SHOT COVERAGE

Shot peening coverage is defined as measure of original surface area that has been annihilated by shot dimples. Coverage is determined according to amount of surface coverage by shot media through nozzle herein media is spayed through surface uniformly and completely. Peening coverage is clearly identified in the standards for each material type and their values are estimated by the help of microscope. Amount of coverage shall be at least %100 per aerospace applications, however, the value changes application to application. Peening coverage is shown in *Figure 5* as different passes.

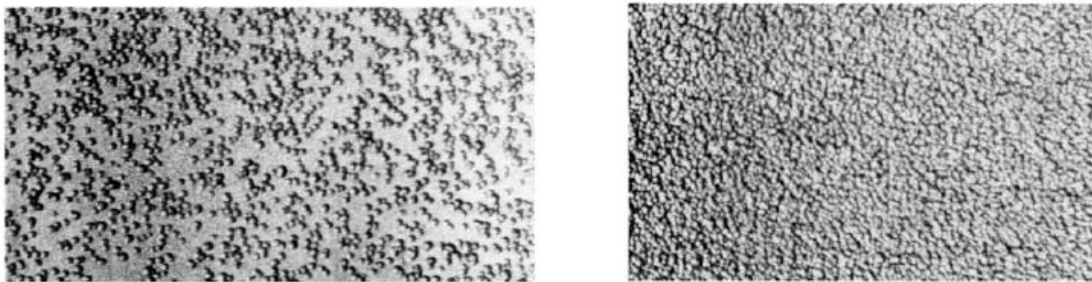


Figure 5 Partial (left) & full (right) coverage cases [27]

2.2.1.3. SHOT MEDIA

By using high quality shot which is mostly round and of uniform size and shape; shot peening operation is performed. Hereby, the critical point is to choose correct shot media in terms of material and size. Also, the shape of the shot media is important because of necessity to obtain smooth spherical impact. In addition to size and shape of the shot media, hardness is also significant. For instance, extreme hardest shot media will scratch the surface of the component and results in premature failure of material under cyclic loading therefore hardness value of shot media shall be optimized. Shot media is classified according to SAE industry standards. Shot peening process is applied to many types of material; therefore, deciding type of shot media for different applications is significant due to severe effect on formed residual stress. As a material, cast steel, glass beads are usually preferred for the applications. The most common one is cast steel shot and it is preferred for the shot peening of ferrous parts and even nonferrous components in case of iron based contaminations. Cast steel shot having hardness of 40-55 HRC is generally used during operation. The other shot media is glass beads that are generally preferred for the nonferrous parts like titanium, aluminum alloys. Moreover, protection of stainless steels against stress corrosion cracking is another candidate for glass beads. In addition, it is used especially for lower intensities.



Figure 6 Examples of different shot media [27]

Shot intensity is directly related and severely affected by the shot size. Generally, it shall be small enough to fill whole parts on surface of the component and this value is preferred to be at least one third of fillet radius. After application, some deformed particle shot medias are carefully discarded by controlled airstream through a falling stream of peening media and others are reused or better quality ones are replaced.

2.2.2. INSTABILITY IN SHOT PEENING

Shot peening is very useful and beneficial process for many practice like crankshafts, gears and springs applications. The scale of shot peening is versatile depending on application to application. It is performed for large scale applications like aerospace components and also applied for tiny scale components such as electronic pieces. The shot peening process is generally preferred to enhance fatigue life of the material by preventing initiation and propagation of cracks on surface of the component. However, the process is also performed to avoid stress corrosion cracking in the corrosive environment that causes failure of the component under applied stress and the atmosphere. Shot peened component enables to endure under cyclic loading in a certain degree; however it precisely increases the life of the material. As a shot peening case, bearing provides in enhancement in the life of component also mobility of material surfaces due to retained lubricants while shot peening operation. Another advantage of shot peening is to assure the closure of pores on the surface of the component that degrades the mechanical properties of the material. For instance, cast products can be improved by shot peening in terms of porosity closure case. Machining marks and any type of surface discontinuities coming from machining process that result in unexpected failure of the component can be prevented by shot peening process. The retained residual stress can be tensile or compressive depending on machining type. Those residual stresses caused by machining process need to be eliminated to acquire safe design life. One of the way to get rid of residual stresses on surface of material is shot peening operation. To control the parameter of shot peening, Almen strip is used that clarifies the amount of severity based on its curved shape. In the case of requirement of peening front and back surface; Almen strip exhibits complex

form; nevertheless, both faces have compressive residual stress at the end of process. Surface finish is occasionally demanded to eliminate the cratered surface state. After shot peening operation, the finishing results in taking off compressive residual stress due to formed tensile residual stress while finishing.

Shot peening operation can also be performed to obtain fine surface finish applications. Demand for surface finish is inevitable for fatigue and stress corrosion cracking to prevent formation of any stress intensifier. To realize this, repeated shot peening operation is required; the first one is performed under optimized peening parameters and the second one is processed to obtain better quality surface finish by handling micro-ball shot peening procedure. To eliminate still retained residual stress after second shot peening operation, electro-polishing can be performed to the material surface that enables to fulfil the desired residual stress homogenously. Surface roughness has detrimental effect on fatigue life and it increases by increasing shot severity. Upon shot media strikes the surface like a hammer, surface roughness of the material will be higher. Hereby, increasing surface roughness leads to decrease in hardness of the component that leads to premature failure under cyclic loading. To provide desired surface finish, suitable shot size and choice of appropriate shot having optimum hardness value are required.

By increasing shot peening severity value, the residual stress gradient will decrease. In addition, residual stress distribution is influenced by surface roughness value. The material having lower surface roughness has higher compressive residual stress at the end of shot peening operation compared to material with higher surface roughness in terms of applied same shot intensity. Similarly, the increasing shot size leads to increased residual stress distribution on the material. Likewise, shot media having higher hardness value will increase residual stress distribution while performing procedure up to certain level.

Under executing fatigue testing, the retained residual stress will start to decrease after certain cycling. Upon shot peened component is exposed to heat treatment process like tempering; the retained compressive residual stress will decrease also. Nevertheless, the

cold working region remains constant although it experiences stress relieve due to tempering process.

2.2.3. PLASTIC DEFORMATION CAUSED BY SHOT PEENING

For smooth specimen that is shot peened homogenously, the stress distribution is shown in *Figure 7* without applying any external stress. In the case of force free condition of the specimen, the formed compressive and tensile zone by shot peening in the material are expected to equal to each other. The area under compressive and tensile zone becomes inverse in terms of sign and their summation are equal to zero. On the other hand, upon applied external stress on the material, the formed stress comes from residual stress plus applied external stress. This part is calculated by simple sum of the stresses in each part of the material. Hereby, the critical point is that the stress on the peened surface that shows compressive residual stress because of shot peening process declines compared to applied initial stress. Consequently, this fact enables to inhibit the initiation and propagation of the discontinuities on the surface of the material and as a result shot-peening improves the mechanical properties especially fatigue life of the component.

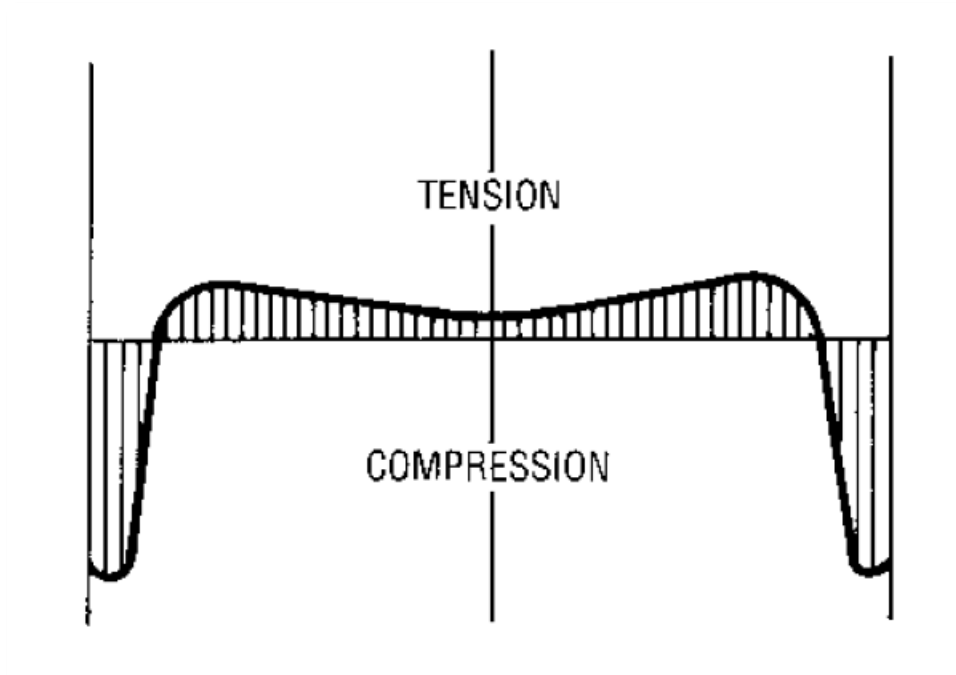


Figure 7 Typical residual stress distribution in the cross-section of the shot-peened material [27]

Basically, the phenomenon behind of cold working deformation caused by shot peening operation and cyclic deformation resulted by fatigue is quite similar to each other. Upon soft materials are loaded cyclically, subgrain size in the microstructure will be reduced due to climbing in the straining. As a result, lattice points in the microstructure will be distorted and dislocation density will increase because of straining; therefore, cyclic hardening forms. On the other hand, when shot peened components that are basically cold worked are loaded cyclically, the agglomerated dislocations resulted by straining are annihilated and subgrain size enlarges. Eventually, the lattice points will be distorted less and number of dislocation density will be less compared to loaded soft materials cyclically and cyclically softening realizes [15].

After shot peening operation, work hardened layer forms on the surface and softened layer forms just below the hardened later. As a result, cyclic re-hardening phenomenon occurs on the surface after softening stage mentioned above during cyclically loading. This

phenomenon clarifies the effect of shot peening on fatigue life. Formed compressive residual stress on surface resulted by hardened layer prevents initiation and propagation of crack on the surface of the component. On the other hand, plastic deformation will be inhomogeneous under cyclically loaded soft materials like stress relieved steel. It will be resulted in formation of micro-cracks and leads to premature failure. By the help of shot peening application, plastic deformation will be homogenous and it creates work hardened surface that avoids formation of discontinuities. Therefore, shot peening is beneficial process for fatigue life of the components.

2.2.4. INFLUENCE OF SHOT PEENING ON FATIGUE LIFE

During cyclic loading, fatigue crack formation is usually observed on the surface of component because of surface discontinuities like scratch, micro notches and surface flaws and also having dissimilar physical and chemical properties of the surface compared to microstructure. Those discontinuities create stress concentration on the surface and result in crack initiation and propagation on the surface. To eliminate detrimental effect of surface under cyclic loading, shot peening application needs to be performed.

The shot peening affects the surface positively in terms of work hardening and retained internal stresses. The first one is provided by formation of micro hardness on the surface. Surface hardness is related with shot severity; in other words, shot velocity coming from nozzle. In this way, nucleation of crack can be postponed thanks to shot peening. It is well known that fatigue crack forms just below the hardened surface after shot peening process or other hardening processes. Other types of hardening process like carburizing or nitriding form internal stress on the surface; however the difference between surface and interior part is so deep in terms of internal stress which means transition from compressive to tensile stress is observed suddenly. This situation creates acceleration of crack under cyclic loading. Conversely, shot peening forms compressive residual stress on the surface and its profile comes down smoothly throughout skin depth. Therefore, this leads to

decreased stress concentration on the transition region and best fatigue performance is acquired by optimized shot peening parameters.

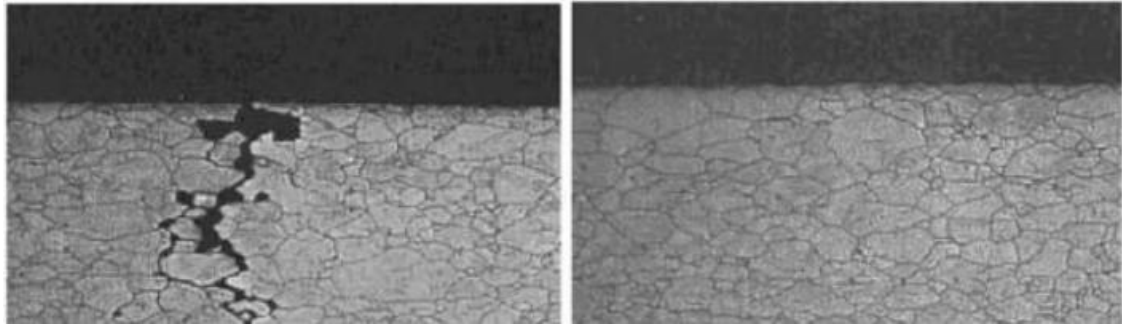


Figure 8 Micro crack formation on the surface: unpeened (left) and shot peened (right)
[29]

The amount of compressive residual stress and formed hardened layer depth are directly effects the life of component. For instance, high strength steels display slowest rate in terms of crack initiation and propagation thanks to optimized shot peened process that leads to optimum compressive residual stress and hardened layer on surface. Otherwise, same group of materials having over peened process that decreases amount of compressive residual stress and insufficient hardened layer on the surface exhibit fast nucleation and propagation of crack; as a result, it leads to premature failure of component.

Fatigue life of component is influenced by structural changes; for example, phase transformation from austenite to martensite for steels is favorable in terms of endurance of material under cyclic loading. Also, hardened of the surface by shot peening operation that triggers the carbide dispersion provides enhancement in fatigue life. By applying shot peening operation, surface condition of the material is severely affected. For instance, surface roughness will increase at the end of process, direction of grains can be altered and forms of micro notches will chance.

To prevent premature failure of the component under cyclic loading, it needs to be performed to prefer high strength materials that have higher strain for endurance or design the component having less stress concentration section on critical parts. This results in enhancement in fatigue life of the component. The previous one involves to choose material having lower fracture toughness and it leads to delay crack nucleation and propagation. The latter one provides less strain requirement on the component to increase the fatigue life or component can be enhanced by applying shot peening operation that forms compressive residual stress on the component. Shot peening is a beneficial process by producing internal stress on the surface of component. It is concluded that even if the design material had chosen as having less mechanical properties, it can be processed by shot peening to increase fatigue life. Shot peening is a beneficial process by producing internal stress on the surface of component. The relationship between the strength of material and formed compressive residual stress after shot peening is proportional to each other. High strength material has higher compressive residual stress after peening process. Therefore, advancement in fatigue life will be higher in high strength material compared to low ones. This phenomena is especially supported around $1E+07$ cycles as shown in *Figure 9*. In addition to this, higher strain hardening is obtained for high strength materials.

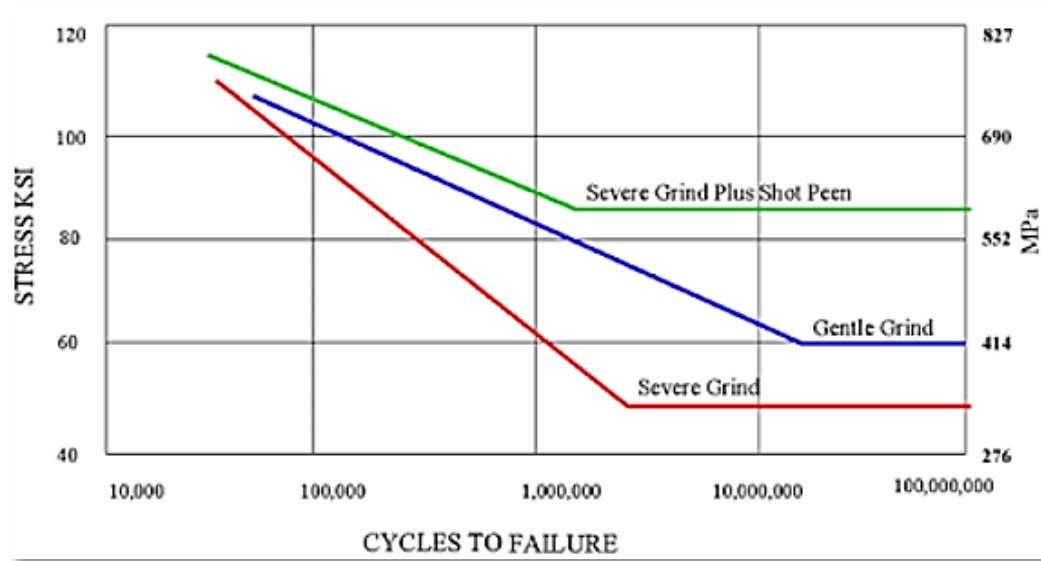


Figure 9 Improvement of endurance limit via shot peening [30]

The formed compressive residual stress may be loosen under random loading condition for especially low strength materials. Maximum compressive residual stress is acquired during peening operation for high strength material. Also, maximum performance of retained internal stress is obtained on high cycle region for strength materials. When we compare the different materials having yield strength in terms of fatigue life, higher yield strength will show higher enhancement in fatigue life and amount of formed compressive residual stress after shot peening operation. This phenomenon is based on aforementioned mechanism that is stated as having higher relaxation under cyclic loading and formed less compressive residual stress for low strength material. Crack initiation and propagation are prevented thanks to formed high compressive residual stress. As a result, higher compressive residual stress will decrease the applied maximum stress value more and enhance the fatigue life.

2.2.5. OPTIMIZATION OF PEENING PARAMETERS TO EXTEND THE SERVICE LIFE

Shot peening is quite favorable process for the industry to enhance fatigue life of component. General type of shot peening operation with considering its parameters will improve the life of component; the critical point is to determine optimized peening parameters. Optimization of shot peening parameters results in higher amount of compressive residual stress forming on the surface of component that presents best improvement. On the other hand, random shot peening operation leads to less improvement in fatigue life or overpeening is also resulted to get less compressive residual stress on the surface of component. Therefore, setting optimum shot peening parameters for any material is inevitable to acquire best fatigue life. Overpeening forms folds on the surface because of extensive strike of shot media that leads to unexpected failure of the component under cyclic loading. Dangers of over peening are indicated in *Figure 10*. For those circumstances, the component needs to be applied surface finish operation; nevertheless, the intended life may not be obtained due to existence of folders coming from previous peening operation.

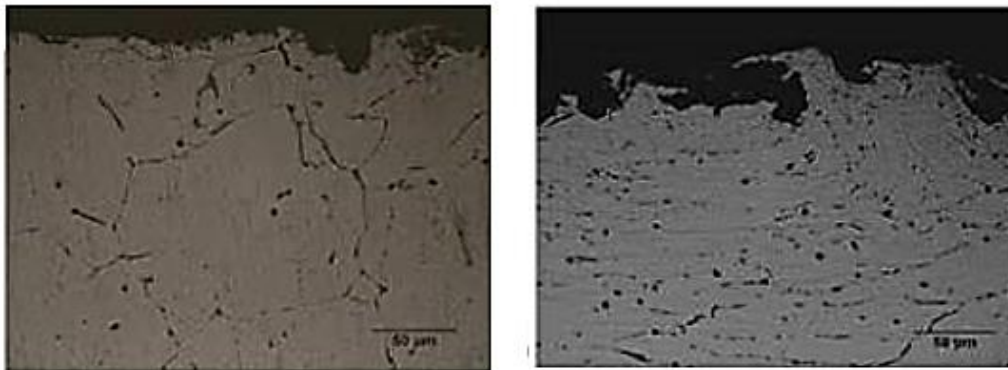


Figure 10 Properly shot peened (left) versus over peened (right) [31]

Shot peening media influences severely the life of component in terms of its weight. For instance, the lighter ones like glass shots enhance the fatigue life of component compared to heavier ones such as steel or other types of alloys. In addition, scatter in the test results

is minimized by using lighter shot media. The heavier shot media is not advised for softer materials to influence the performance of component negatively. Shot media needs to be relatively softer than material peened and other parameters shall be determined accordingly. Chosen random parameter may have detrimental effect on fatigue life and even it encourages the initiation of fatigue crack. Therefore, each parameter is critical and meticulously evaluated before application. Hereby, the maximum performance is obtained re-process of the peened component by eliminating surface flaws by polishing firstly and then re-peening by using lighter shot media that makes component hardened for initiation of fatigue cracks under cyclic loading.

Fatigue life of the component and crack closure mechanism during determination of long crack threshold depend directly on shot-peening operation. Naturally formed cracks during manufacturing process experience plastic deformation on the wake of crack thanks to shot peening process. The formed compressive residual stress on the wake of crack improves the crack closure mechanism and da/dN rate will decrease under constant loading case. As a result, crack propagation will be delayed thanks to enhancement in crack closure mechanism. Hereby, the critical point is that complete crack size shall be peened not only tip of crack to enhance the fatigue life. During performing da/dN test of CT (Compact Tension) or SEB (Single Edge Bending) specimen type, the enhancement in crack closure is acquired by shot peening operation through notch. By complete peening through the crack size, work hardened crack and retained internal stress delay the crack propagation; as a result, the applied load shall be increased to advance the crack. The crack closure is favorable mechanism that delays the propagation of crack. Shot peening is one the best process to retard the crack propagation rate by advancing the crack closure. Shot peening through crack size resulted in plastically deformed crack wake. Moreover, improvement in crack closure directly influences threshold stress intensity factor (ΔK_{th}) during da/dN test.

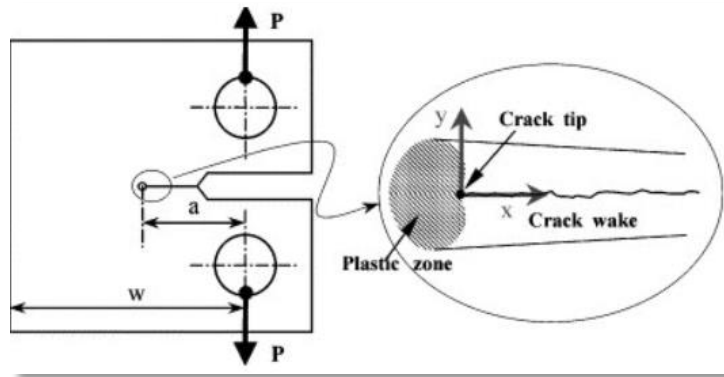


Figure 11 Improvement of crack closure by shot peening [32]

Crack growth behavior of the metallic components is judged through Paris equation. It is defined according to the 2nd stage of the da/dN curve. Crack opening stress intensity factor will increase because of shot peening through crack size. After shot peening operation, crack nucleation and propagation will delay due to plastically deformed crack wake. To open the crack mouth, higher stress levels need to be applied. Therefore, it could be concluded that shot peening process enables to have lower crack growth rate thanks to improvement in crack closure.

The size of precipitation within the microstructure severely affects fatigue crack initiation and propagation rate. Equivalent plastically deformed hardenable alloys demonstrate different behavior in terms of plasticity because of distribution of precipitates. Hereby, inhomogeneous distribution of plastic deformation is observed in materials having smaller size of precipitate particles. This circumstance supports easier dislocation motion since smaller size of particles is likely sheared out by dislocations and it requires lower stress levels. In addition, inhomogeneous plastic deformation is also observed in lower stacking fault energy and large grain size microstructure. Upon increased number of slip in smaller precipitate distributed as random leads to decreasing the rate of nucleation of fatigue crack under cyclic loading. Conversely, larger precipitates provide homogenous slip mechanism that higher stress level is required for dislocation motion. In conclusion, homogenous slip distribution in large precipitates results as improvement in fatigue life

due to retardation of crack nucleation. The crack nucleation in larger precipitates for hardenable alloys is advocated by homogeneous slip distribution; however, it provides more crack propagation rate under constant load. Therefore, the critical point is that it shall be obtained optimum life of material by balancing initiation and propagation of fatigue. It is performed by homogenous slip distribution to improve the initiation and plastically deformed alloys having inhomogeneous deformation microstructure to enhance the crack propagation rate. These common requirements are supplied by shot peening process that provides inhomogeneously deformation through shot strikes. By the help of shot peening, many dislocation movement is observed on the surface plastically deformed. Agglomerated dislocations interact with each other without enabling sharp slip. This results in homogenous slip distribution on the deformed zone and it delays the nucleation of the fatigue crack. Even if the crack is nucleated under cyclic loading, formed compressive residual stress avoids the movement of dislocations and as a result it delays the propagation of fatigue crack.

2.2.6. SHOT PEENING OVERVIEW

Shot peening operation depends on many parameter mentioned above and optimum parameters are required to obtain best performance of material. During determining optimum parameter, their interactions are also taken into consideration. Shot peening process is favorable for any type of materials without considering hard or soft in terms of advancement in fatigue life since it retains compressive residual stress on the surface by work hardening and delays the nucleation and propagation of fatigue crack. Hard materials experience hard surface layer and soft bulk structure after shot peening process, on the other hand, soft materials are exposed to homogenous deformation distribution on the microstructure that enables to lower rate of crack propagation. The soft material has homogenous plastic deformation and homogenous slip distribution after shot peening operation and it results enhancement in crack nucleation under cyclic loading. Shot peening operation contributes to low and high cycle's region of SN curve for low and high strength materials by work hardening surface. Hardened surface layer thanks to strain

hardening provides compressive residual stress on the surface of component and retained internal stress leads to enhancement in fatigue life. Crack propagation rate is reduced by shot peening operation because of closure effect phenomenon which is caused by plastically deformed crack wake under cyclic loading.

2.3. EFFECT OF RESIDUAL STRESSES ON FATIGUE LIFE

Fatigue life is affected by several factors like microstructure, environment, geometry of sample and residual stresses. First of all, microstructure of the material directly influences the life of material. For instance, smaller grain size shows higher strength and they have enhanced fatigue life compared to larger ones. On the other hand, larger grains exhibit increased fatigue life at elevated temperature condition. For materials containing impurities, second phases and precipitates, fatigue life is improved due to hindering movement of fatigue crack. In addition, fatigue life is enhanced in case of phase transformation under cyclic loading.

Through applying surface treatment methods, fatigue performance of the material enhances severely. It is well known taking place of common failures at the surface of components; therefore, compressive residual stress at the surface layer shall be introduced to resist formation of crack. Existence of discontinuities at the surface facilitates formation of possible crack initiation zones under cyclic loading. As a result, formed residual stress retards crack initiation and propagation period. Thus, contribution of compressive residual stress formed at the surface layer on fatigue performance of engineering components is priceless. In the light of this information, shot peening, carburizing or nitriding etc. are common techniques in the industry to form compressive residual stress to enhance fatigue life of material. Beside conventional techniques, laser shock peening and low plasticity burnishing start to become intriguing.

On the other hand, formed tensile residual stress deteriorates fatigue performance of the engineering components. After machining operation, generally tensile residual stresses form at surface layer of material. Existence of tensile residual stresses simplifies initiation

and propagation period of cracks. Crack nucleation sites on the microstructure are extrusion and intrusion of slip bands, grain boundaries and formed micro-notches. Distorting surface quality caused by any operation results in earlier crack nucleation and propagation. Upon cyclic loading, major part of the fatigue life is because of initiation of crack. Therefore, improving surface quality usually will increase the life of material by retarding formation of initial crack.

The form of material is critical in terms of fatigue life. Fatigue life is improved in case of loading in the direction of manufacturing process like rolling, extrusion and forging; conversely, transverse life exhibit less fatigue life. Other types of processes like cold working, shot peening retains compressive residual stress on the surface of material that leads to hardened surface layer to prevent nucleation and propagation of cracks and as a result it improves fatigue life. Some processes form tensile residual stress that endorses crack nucleation. In addition, surface roughness influences severely the fatigue life. The processes like forging and punching create very rough surface that leads to reduced fatigue life. To avoid the surface roughness effect, polishing process like eletropolishing is advised.

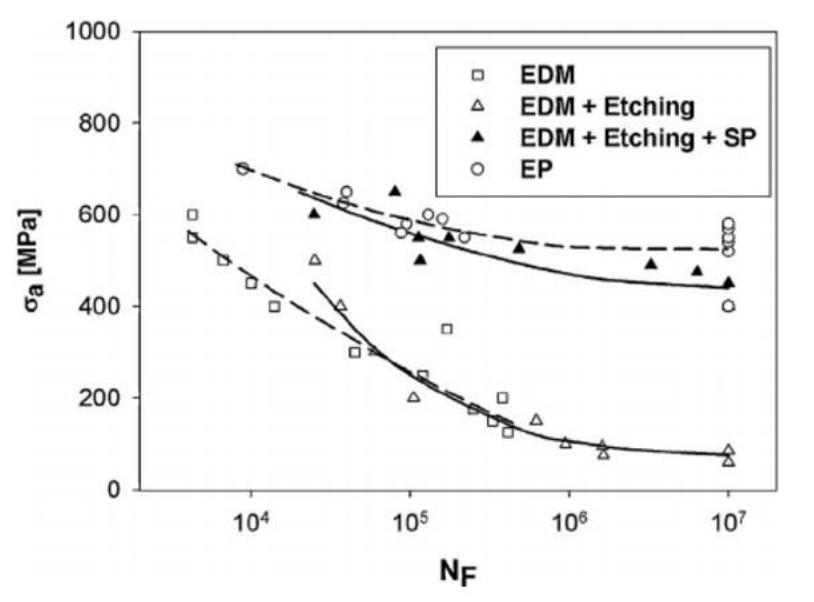


Figure 12 Enhancement of fatigue life via polishing [33]

Another important factor is geometry of material. Components having holes and notches show less fatigue life due to increased stress concentrations on the discontinuities. Under same loading condition, notched specimens show less fatigue life compared to plain one. The atmosphere of the operation affects directly the life of material. In aqueous and corrosive environments, fatigue life will reduce due to pitting under cyclic loading. As a result, crack propagation rate will increase and cause premature failure. Also, fatigue life will lessen at elevated temperature condition due to creep. Loading regime is also significant in terms of fatigue life. Uniaxial loading case is better than multi-axial loading. Moreover, negative mean stress improves the fatigue life especially at high cycle region compared to positive mean stress. To sum up, several factors provoke the crack nucleation and propagation under cyclic loading.

2.4. MAGNETIC BARKHAUSEN NOISE METHOD

The material properties severely depend on microstructure and the composition of the material. It is critical to evaluate all the affecting parameters during measurement

especially magnetic properties of the material not to get incorrect data coming from MBN signal. The microstructure of the material significantly impresses the value of permeability and as a result it affects magnetic property. Depending on filling d-band; ferromagnetic feature changes. For instance, pure iron and nickels are heavily ferromagnetic and partial concentration of iron and nickel becomes less ferromagnetic. Also, the crystal structure of the material that whether it is directionally dependent and orientation of the material affects the magnetic properties of the material. For instance; highly anisotropic materials display high magnetic anisotropy. Moreover, the structure of the material like face centered cubic or body centered cubic affects the magnetic properties of the material. Also, alloying element is crucial for the magnetic properties especially carbon content in the steel affects the movement of domains in the structure. Second phases, precipitates and amount of carbon content have pinning effect on movement of magnetic domains under applied magnetic field. As a result, magnetic property is unique for the materials in terms of variations in the property.

During manufacturing of the material; some discontinuities like grain boundaries, inclusions, dislocations, precipitates are formed and those discontinuities prevent movement of magnetic domains in the microstructure. Also, grain size of the microstructure affects the movement of the domains. For instance, smaller grains which mean higher grain boundary in the microstructure have higher pinning effect for domain walls. The phase boundaries have pinning effect and increase coercivity and enlarge hysteresis loop that cause harden magnetically. For example; martensite magnetically is much hardened than ferrite due to higher phase boundaries in the microstructure. If the inclusions or precipitates show non-magnetic properties, they pin the magnetic domain wall movement and increase coercivity and magnetically hardens the microstructure. Heat treatment causes microstructural changes and alters the magnetic properties of the material. For instance, the welding region has heat affected zone where important changes in the microstructural are observed and the residual stress in the welding zone is directly measured by using MBN data. Also, plastically deformed materials experience dislocation

entanglement in the microstructure and this results in higher pinning effect on magnetic domain walls.

Martensitic transformation in the steels causes both microstructural change and also retained strain because of nature of the microstructure. Therefore, this structure type has two different effects on the magnetic property. First one causes pinning effect and the second one affects relative permeability due to retained residual stresses. Both of them directly affect the magnetic properties of the material concurrently. In addition, change in the characteristic of the material like content difference, microstructural change and property difference varied from region to region make calibration difficult.

The magnetic hysteresis curve is acquired the change in the magnetic flux density (B) versus magnetic field (H). The hysteresis curve is affected by magnetizing field, magnetizing frequency, temperature, composition of the material, microstructure and formed residual stresses.

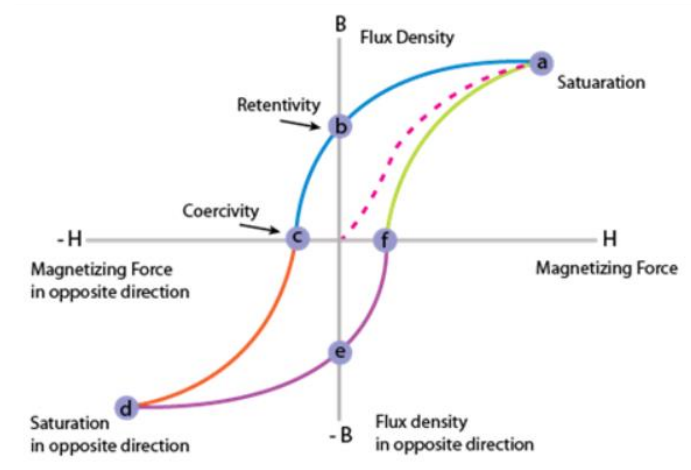


Figure 13 Magnetic hysteresis curve [21]

The area covered by the hysteresis curve indicates the energy loss. Many material properties are originated by hysteresis curve such as coercivity, remanence and permeability. The coercivity is described as measure of the reverse field needed to drive the magnetization to zero after being saturated. The remanence is described as measure of

the remaining magnetization when driving field is dropped to zero. Permeability is the property of material that describes the ease with which a magnetic flux is established in the material. Theoretically, acquiring the ideal saturation involves superior magnetic field.

When the magnetic flux equals to zero which means there is no flux outage, coercive force values are measured as detached of demagnetization effects. By the way, coercive force is affected by the microstructure of the material like grain size and the second phase particles. Coercive forces are severely influenced by the pinning effect of the discontinuities.

The hysteresis curve is garbled by applied or formed stresses; as a result, the related parameters those are coercivity, remanence and permeability are affected substantially. Full hysteresis curve evaluation of the material is generally not convenient due to not generating the uniform fields. In addition to this, obtaining full saturation levels is out of scope because of the existence of demagnetizing fields. By handling low field magnetic susceptibility measurement, the magnitude and direction of the intended stress could be identified.

Magnetic Barkhausen technique provides easy, rapid and totally non-destructive method and practicable for in place evaluation on industrial parts and structures. Nevertheless, the measurement of the component becomes too sophisticated due to their high sentiment to internal stress under applied magnetic field. Also, they are affected by other factors like microstructure of the component that makes inconvenient of precise data interpretation. The important advances have been achieved over the last decades on behalf of MBN method to provide practical measurement by preventing the experienced difficulties due to material's nature.

Barkhausen jumps resulted by distinct changes during magnetization are evaluated by the help of the MBN technique. Barkhausen jumps can be observed as steps in the hysteresis curve and are reflected to be straight proof for domain wall movement during this magnetization process as shown in *Figure 14*.

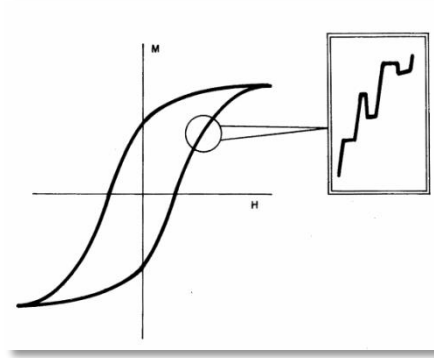


Figure 14 Magnetic hysteresis loop and Barkhausen jumps [19]

Measurement parameters and the material properties influence the shape and size of the MBN signal generated during magnetization. As a result of the MBN signal as electromagnetic diminution, the skin-depth procurement of the MBN signal is hedged to the near-surface region of approximately less than 1mm, but this fact strenuously is bound up with the magnetic excitation frequency and permeability of the material.

The characterization of microstructural changes caused by heat treatment processes like tempering and aging is latterly being utilized by the help of the MBN technique. For instance, estimation of hardness and case-depth alterations in case-hardened steels, evaluation of surface and subsurface residual stresses, procurement of texture orientation, estimation of onward fatigue damage aggregation, procurement of grinding damage in a different type of ferromagnetic steels might be exemplified in the scope of MBN technique.

The temperature affects the results of MBN signal during measurement. Principally, electronic hardware shall be stable. Variation in the material properties coming close to Curie temperature and variation in the electrical resistivity of the component affect the consequence of the measurement. Before starting the measurement; system shall be turn on position for a while for stabilization. In this way, potential changes in the system can be prevented. The significant point is that all samples shall be identical in terms of temperature and at least 3°C deviation can be allowed for each specimen. The reference

sample can be preferred before measurement by hindering change in thermally induced physical property on the material. The magnetization decreases in very slow rate until Curie temperature where increment in rate becomes very fast. Moreover, magnetic permeability becomes zero at Curie temperature.

Rather than using MBN technique, X-ray Diffraction and Hole Drilling methods might be an option for residual stress measurement.

Ferromagnetic materials comprise the magnetic domains that those domains are aligned in parallel in terms of entire atomic magnetic moment vectors. 90° and 180° domain walls separate contiguous magnetic domains in ferromagnetic steels.

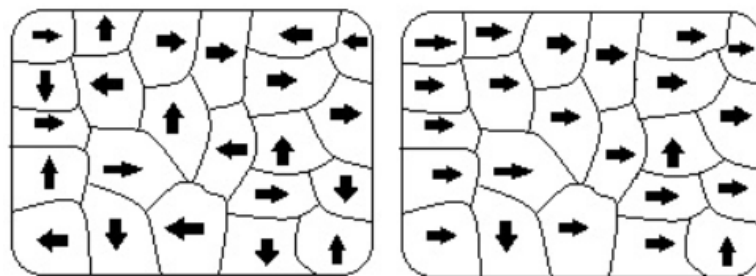


Figure 15 Representative magnetic domain: Unmagnetized (Left) and magnetized (Right) [20]

While a ferromagnetic material at which orientation of entire domains is at a venture and not magnetized yet is subjected to an exterior varying magnetic field, the magnetization that is also expressed as total magnetic moment per unit volume in the material rises in the direction of the applied magnetic field.

The primary section of this magnetization process encloses the irreversible movement of magnetic domain walls by handling different types of obstacles such as grain boundaries, second phase precipitates and other types of discontinuities formed during manufacturing process of the material. On account of this, the phenomenon of hysteresis process is precisely based on the irreversible movement of domain walls.

A number of convenient sense should take into consideration before the Magnetic Barkhausen measurements. Primarily it is should be seized how the knowledge is to be evaluated during measurement and it should be recovered the stress distributions on the magnetized material. For instance, which type of stress or moment is applied to the material should be identified before Magnetic Barkhausen measurement. The present knowledge will affect the conditions to determine the optimum calibration.

In addition to this, the present knowledge will impress which locations is more critical to take measurement, the selection of appropriate probes, and which measurement properties should be considered to acquire optimum measurement results. Likewise, whether the component had been operated by the surface treatment processes, e.g. shot peening operation, the optimum measurement parameters shall be specified by considering stress profile and skin depth state during data gathering. The thickness of the specimen may also influence the measurements made. In the given cases, the required parameters should be determined to acquire the correct data analysis and stress state; otherwise it could be measured higher or lower surface stress depending on chosen measurement parameter on the surface of the given material. Moreover, the thickness of sample and formed high surface stresses caused by machining operation may affect the measurements.

The selection of probe procedure shall be decided minutely according to geometry of the component and of course accessibility of the probe and a suitable apparatus is required for the nonlinear geometries to be ensure that measurements showing parallelism among each evaluation. The purpose is to settle the probe justly orthogonal to every measurement state. Then the magnetic moment vector is aligned according to the applied magnetic field. In this condition, internal stresses and discontinuities change the orientation of the magnetic moment vector. For instance, steels show positive magnetic moment vector on the applied tensile stress direction; on the other hand, nickel shows negative magnetic moment vector that is aligned parallel on the applied compressive stress direction to reduce their energies. Therefore, magnetic hysteresis curves are decided according to underling stress tensor of the material and magnetic domain distribution.

Formed residual stress on material microstructure or applied positive or negative stress severely affects the orientation of the magnetic domain movement. As a result; this keenly impresses the magnetization process.

The magnetization process is also strongly influenced by microstructural features such as dislocations, grain size, second phase precipitates, non-ferromagnetic phases as well as the internal retained stresses. In polycrystalline material; the grain boundaries are the regions of magnetic discontinuity because of different crystallographic orientation and easy magnetization direction of contiguous grains. The magnetic free poles at the boundaries create a demagnetizing field and therefore it would behave like an obstacle to wall movement of domain.

As a rule, it is taken into account that the grain size and its distribution would affect movement of domain wall by changing the free path of the displacement. As a result; it directly affects the magnetization process. Like this, the presence of any inclusions which are non-ferromagnetic and second phase precipitates pin the domain walls and prevent the movement of domains. Also, the size and distribution of second phase particles affect the magnetization process directly.

Upon a tensile stress is applied to materials such as iron and ferritic steels, they are disposed to align their magnetic domain along the applied stress direction and therefore magnetic domains are easily magnetized along the tensile stress direction; on the other hand, if the compressive stresses are applied to the materials; they incline to align their magnetic domains perpendicular to the applied stress direction; as a result magnetic domains are hardly magnetized along the compressive stress direction as exhibited on *Figure 16*.

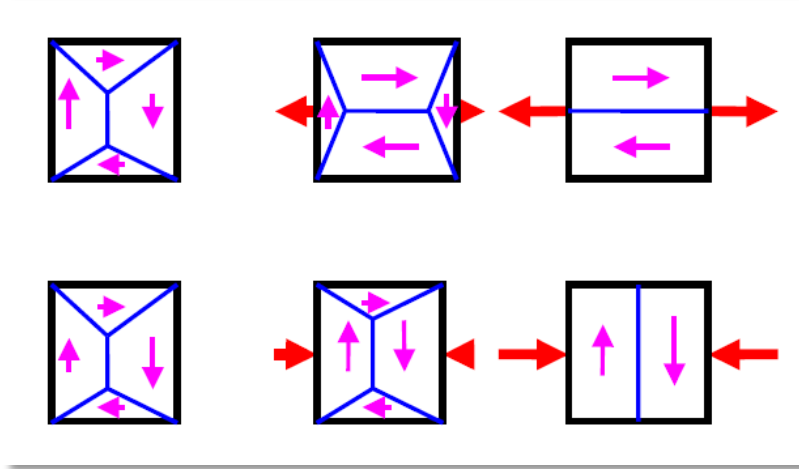


Figure 16 Orientation of domain wall with respect to applied stress: $\sigma < 0$ (middle), $\sigma = 0$ (left) and $\sigma > 0$ (right) [4]

During magnetization process, the response of aligned magnetic domains is pretty dissimilar and complex for every material, especially they are interdependent to each other in behalf of microstructure and stresses state.

2.4.1. MBN DEPTH EVALUATION

Magnetic Barkhausen Noise measurement is basically divided into two categories that are higher and lower excitation frequency MBN for different applications. Firstly, higher excitation frequency that is higher than 10 Hz and MBN frequency range alters between 2 to 1000 kHz that ensures higher external magnetic field. On the other hand, lower excitation frequency usually presents for lower than 1 Hz and frequency range is examined between 0.5 - 100 kHz for MBN measurements [4].

The MBN measurement system comprises in an electromagnetic yoke and a pick-up coil. The resolution of the measurement depends on the size of the instrument. The high excitation frequency encloses lower applied external magnetic field strength and hence the measuring instrument shall be made smaller. This setting is generally performed for approximately 6 mm within the surface of the examined material and roughly 1mm

resolution presents. On the other hand, low excitation frequency encloses higher applied external magnetic field strength and hence the measuring instrument shall be made larger. This setting is generally performed for approximately 20 mm within the surface of the examined component.

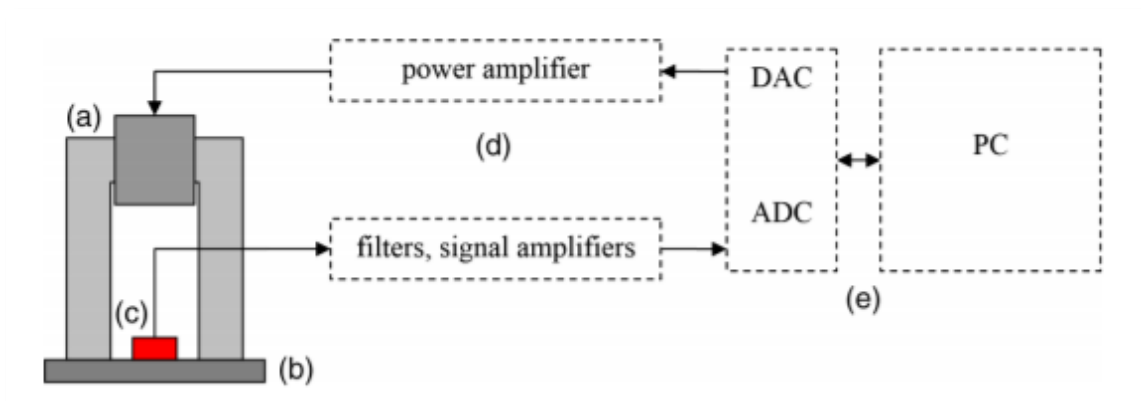


Figure 17 Schematic MBN system: (a) electromagnetic yoke; (b) specimen; (c) coil [23]

To be able to determine maximum skin depth from the surface, it needs to be estimated the change in the material properties throughout inside direction. Skin depth usually changes with permeability of the material, electrical resistivity of the test material and frequency of the MBN signal. Moreover, magnetic field strength decreases with the throughout direction from the surface of the material. As a result, MBN signal alters with depth distance.

Magnetic Barkhausen Noise value is severely influenced by different type of parameters such as the value of excitation frequency of external magnetic field, the choice of investigated frequency range, geometry of the component, the size of electromagnetic yoke and sensibility of the pick-up coil. Actually, it does not exist any acceptable equation or formula to determine the skin depth of the component coming from MBN signal. As a consideration, the skin depth shall be lower value with applied high frequency signal because it enables having lower magnetic field penetration compared to low frequency measurement. Nevertheless, the skin depth estimation becomes difficult for roughly 10

microns from the surface with high frequency measurement; however, this value becomes much higher by low frequency measurement. The actual skin-depth may alter by the performed instrument, probe and parameters operated during measurement.

The measurement of skin depth cannot be precisely acquired as mentioned above due to the influence of surface properties on the Magnetic Barkhausen Noise signal. To clarify this fact, some examples can be served. For instance; formed residual stress throughout the depth, substantial amount of surface roughness, formed oxide layer on the surface of the component and any machining process like grinding severely affect the MBN measurement for high excitation frequency. During the measurement of MBN signal, those factors shall be evaluated. On the other hand, the measurement of skin depth value is much higher for low excitation frequency measurement. Due to this fact, the change on the surface of the component cannot be taken into consideration for low frequency measurement. Hence, low frequency measurement is usually preferred to determine the skin depth for subsurface applications.

2.4.2. MAGNETIC BARKHAUSEN NOISE SYSTEM

The Magnetic Barkhausen Noise probe is basically formed by two parts: Electromagnetic yoke and a pick-up coil. The benefit of the electromagnetic yoke that is fabricated by a soft ferromagnetic core material is to generate magnetic flux with low hysteresis loss. The function of electromagnetic yoke is to maintain excitation. In this point; it shall be properly contact space between surface of the component and probe to minimize air gap that is the reason of demagnetization and increase magnetic field penetration.

There are basically two critical parameters to determine magnetic field strength: The number of coil turns and applied current in the electromagnetic yoke. By optimizing number of coils and the current; appropriate electromagnetic yoke can be identified. Hereby, current could not be higher than 1.5A to extend lifespan of electromagnetic yoke; generally 1A is preferred. Magnetic field strength is adjusted according to number of coils by keeping current constant. If the number of coil increases; it is concluded higher

magnetic field strength that results in getting maximum hysteresis loop by closing saturation level. In this condition; it requires higher electromagnetic force that makes difficult to apply magnetic field at higher excitation frequencies. Thus, obtaining higher magnetic field strength and deeper skin depth are advised by lower excitation frequencies.

Electromagnetic yoke is fabricated by the soft ferromagnetic core such as pure iron to obtain higher magnetic field strength in low excitation frequency measurements. By choosing ferritic steel for electromagnetic yoke core and smaller number of coils, high frequency measurements are performed. On the other hand, higher number of coils that results in larger size of electromagnetic yoke enables higher magnetic field strength for low excitation frequency measurements.

During performing MBN measurement at high excitation frequency which means higher increment in delta magnetization; it is resulted as higher MBN voltage jump in the hysteresis curve. In addition to this; high excitation frequency enables to high frequency range for MBN measurement that facilitates smaller number of coils due to the feature of easy detection of the signal. On the other hand; delta in the magnetization is smaller for low excitation frequencies during MBN measurement. Therefore; it requires high number of coils to gain deeper the signal from surface of the component. As a result; number of coils in low excitation frequencies is larger than relatively high excitation frequencies. To obtain sensible signal and get smaller size by the measurement; thin copper wire shall be preferred as coil material. In some application; size of the pick-up and electromagnetic yoke make difficult to realize the MBN measurement; thus, the size of the instrument shall be taken into consideration before starting the MBN measurement.

2.4.3. MBN OPERATION METHOD

The MBN measurement system primarily consists of signal generator, power amplifier, signal amplifier and data acquisition system. The device principally works out by connecting signal generator to power amplifier that provides necessary power and operates the electromagnet. To obtain needful frequency and amplification; pick-up coil

is connected to power amplifier. Desired MBN signal is generated by the help of data transfer system that is generally PC. As a result; diverse data profile such as MBN profile, total RMS can be plotted by the generated signal. According to the excitation frequency range, the size of electromagnetic yoke and number of pick-up coil shall be determined. Based on frequency range; signal amplification would be different. For instance; lower signal amplification shall be preferred for high excitation frequency measurement. To be able to obtain best signal detection, the pick-up coil that is manufactured with ferritic steel shall be in good contact with surface of measured sample.

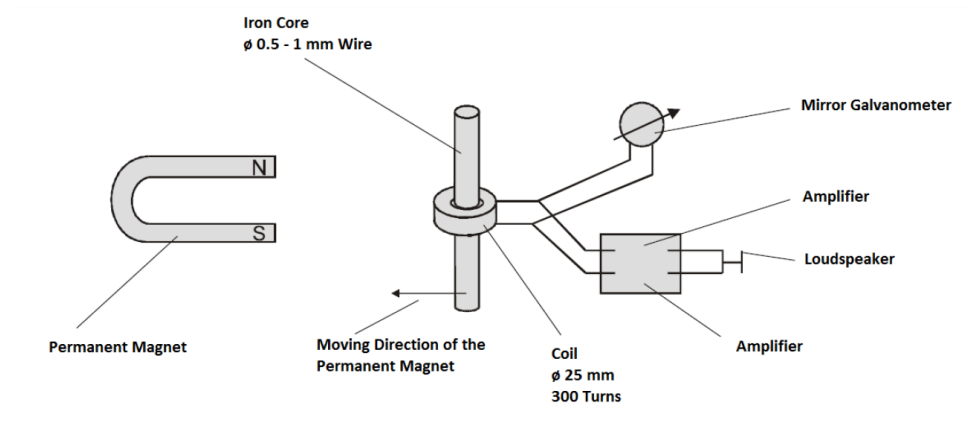


Figure 18 Observation of Magnetic Barkhausen Noise [38]

The required amplification and frequency range are determined according to type of material. To acquire reliable MBN data; desired amplification and magnetization cycles should be determined with the reference sample by achieving different trials. Finally, the MBN measurement is performed by identifying magnetization and amplification values and the diverse MBN parameters like RMS voltage versus residual stress are plotted.

Ferromagnetic property shows diversity for every type of material since it depends on microstructure that is characteristic feature of each material and also retained stress on the material; therefore, calibration before measurement is inevitable for each type of material. By performing calibration, deviations affecting ferromagnetic property can be correlated

to obtain precisely reliable MBN data. For instance, when different heat treatment processes are exposed to same material; the ferromagnetic property for each case becomes different due to microstructural change. To acquire correct MBN data, calibration is required for each heat treatment; as a result, the calibration is unique for each case.

Magnetization depends on magnetic field strength in the material and it is affected from various parameters. For instance, applied field strength and the size of electromagnetic yoke directly impress the magnetization. Moreover, the geometry of the material is a significant factor affecting magnetization. The demagnetization effect of the component is linked to length to width ratio and this diminishes the field strength of the material that reversely affects the magnetization. In addition to this, surface area of the measured samples is critical in terms of magnetic field strength. A larger surface area of the component which means higher flux concentration is present diminishes the magnetic field penetration depth. When those parameters are considered; calibration is inevitable for each material to get best correlation.

It is hard to estimate magnetic response in the material under applied magnetic field due to involving lots of variations in the characteristic of the material. The purpose shall be able to obtain maximum magnetization during the measurement that provides maximum MBN signal and therefore maximum material data and feedback. To practice this; it entails the maximum magnetic field strength and as a result highest saturation level is achieved in hysteresis loop. In order to measure material property; optimum level MBN signal that is enough to acquire signal is needed and it is provided by applied magnetic field. Magnetic field diminishes progressively to desired level that enables to determine the frequency range for the user who confidentially comments the magnetic property of the material.

2.4.4. ACCURACY IN MBN SYSTEM

By ensuring the MBN measurement parameters and other factors that are assumed as unaffected for each case, the measurement can be replicated for many times. Therefore, accuracy of the system is quite reliable. The verification is simply performed by observing previous measurement data. If the signal deviation occurs during measurement; the common reason can be air gap between probe and the specimen. As a result; MBN measurement is pretty confidential for industrial application in terms of accuracy. When MBN measurement is performed for identifying a certain material characteristic; the accuracy problem may appear due to effect of more than one material characteristic. For the given cases, accuracy can be assured by increasing MBN parameters that provides to separate the material property alone.

The MBN method may provide an easy way to determine residual stresses in the industrial products, as an alternative way to the traditional techniques. However, it is quite important to ensure accuracy during MBN measurement. Therefore, mechanism behind the system and critical items mentioned above shall be comprehended particularly. In this manner, inspector may operate the system without consisting of any doubt in terms of MBN signal.

Before starting the measurement; surface of the component shall be purified by the chemical fragment like rust especially for high excitation frequency measurement. Also, the component shall be demagnetized if it is magnetically hard. The contact surface between component and the probe shall be assured to obtain reliable MBN data. Calibration point is quite important and shall be performed by the reference sample before measurement for different material and geometries. It should be determined frequency range according as desired stress profile on the component.

The MBN method provides to determine retained residual stress of the ferromagnetic material by the help of magnetic signal. It is essentially divided into two categories during the measurement of MBN technique. The first one is low excitation frequency and the other one is high excitation frequency measurement. Low excitation measurement enables to collect MBN data from deepest part of the component. On the other hand, the high

excitation frequency provides to pick up the MBN signal on the surface of the component. The low excitation frequency requires applying higher magnetic field. Hence, it needs larger MBN system to get higher magnetic field and slower measurement. However, the high excitation frequency entails applying lower magnetic field. Hence, it demands smaller MBN system to get lower magnetic field and faster measurement.

It is critical to establish the required parameters before measurement for both cases due to variation in MBN signal. Firstly; appropriate MBN system shall be chosen and parameters shall be optimized to get maximum reliability of the MBN data. Later, calibration with established reference sample shall be performed due to the nature of the each ferromagnetic materials. Nevertheless, it can be less performed especially for the residual stress measurement with high number of specimens consisting of same material. However, calibration is inevitable to interpret the mechanism under behind of the MBN for specific studies.

2.5. DETERMINATION OF RESIDUAL STRESS BY MBN TECHNIQUE

If the ferromagnetic material is exposed to an altering magnetic field, the magnetic flux density changes in which distinct steps are observed during magnetization. As a result, the magnetic domain walls come across the interior discontinuities under magnetic field. To be able to movement of magnetic domains, the domain walls shall surmount those discontinuities to rise the magnetization in the exterior direction of magnetic field. These distinct changes in the hysteresis curve is described as “Barkhausen jumps”. It shows noise-like voltage pulses corresponding time derivative of the actual magnetic flux changes during magnetization. The noise like voltage pulses were first investigated by Barkhausen, and this fact is acknowledged as Magnetic Barkhausen Noise (MBN). The Magnetic Barkhausen noise is severely affected by the material properties like composition of the material, microstructure and also formed residual stresses.

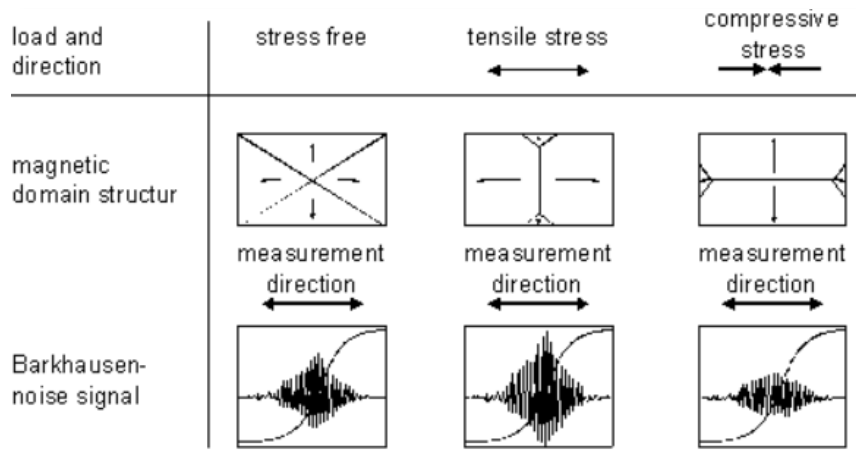


Figure 19 Variation of MBN voltage pulses with stress [22]

The alteration of MBN signal for the ferromagnetic material is caused by the diverse parameters under magnetic field. Magnetic Barkhausen Noise signal is plotted by the root mean square of the MBN voltage versus applied magnetic field or current which is applied to the electromagnet during magnetization. By analyzing the changes in the number of peaks, height of the peak or peak position of the MBN signal, material properties such as composition and microstructure could be interpreted. In addition to this, the total MBN energy and RMS value of the overall MBN created by numerous cycles are the significant indicator to identify the material properties.

MBN measurements can be performed by operating a low magnetic excitation frequency that is in the range of 0.1Hz to 1Hz with the frequency range of 0.5 to 100 kHz to analyze of the MBN signal. The second option is to perform the measurement by operating a high magnetic excitation frequency which is in the range of 10 to 125Hz with the frequency range of 10 to 1000 kHz. In the industry; MBN measurement apparatus generally exerts by the high frequency excitation at 125Hz and analysis in the range of 70-200 kHz [4].

The idea is that low magnetic excitation frequency enables obtaining relatively high skin depth measurement; however, high magnetic excitation frequency provides to measure low magnetic field strength of the material on the surface such as determination of

compressive residual stresses after shot peening process. Therefore, determination of excitation frequency alters according to the performed application. For instance, total RMS value or MBE energy is analyzed by operating high magnetic excitation frequency.

The major advantage of MBN technique is to provide detecting any change in the material properties like microstructure caused by the processes during manufacturing. To be able to understand the mechanism behind of the operation, MBN is required to reveal the material properties. For instance; the grain size, alloying elements, density of the material and arrangement of dislocations, size and volume fraction of secondary phases, applied residual stresses, creep damage and fatigue damage can be exposed by the help of MBN technique. In addition to this, mechanical properties can be identified by the MBN measurements. For example, martensitic steel shows low MBN value due to the increased number of dislocations that those dislocations have pinning effect under magnetic field by hindering the movement of magnetic domains. On the other hand, tempered steel shows high MBN value because of decreased number of dislocations that provides easy movement of magnetic domain walls. Moreover, the grain size, second phase particles severely affect the movement of magnetic domains. If the microstructure has larger grain size which means having wide space to be easily movement of magnetic domains without prevention of the movement. The size of the precipitates inside the microstructure directly influences the movement of magnetic domains. Volume fraction of the second phase particles affects the MBN level as specified in the case of size of the precipitates. Also, phases in the microstructure directly influence the MBN value; for instance, austenite phases are lower MBN value rather than martensitic phase relatively. As a result; MBN permits to obtain significant information about material properties.

2.6. RESIDUAL STRESS ANALYSIS BY X-RAY DIFFRACTION

In analysis of XRD residual stress measurement; formed strain in crystal lattice due to machining or other types of process is basically evaluated. Achieving strain in the lattice gives interpretation of formed residual stress on the material. Hereby, elastic distortion of

the lattice is counted as linear. It is well known that formed stress on the material is not evaluated immediately; it requires external measurement in which it is related with strain reading on the material. Acquiring strain on the material that is based on displacement on gage length of the specimen and information coming from cross sectional area of the specimen gives interpretation of applied stress on the material. Magnetic Barkhausen Noise and some destructive techniques present limited or mixed knowledge on interpretation of residual stress. Herein, mechanical methods enclose some constrains like specimen dimension and formed stress field etc. Moreover, this technique is destructive and no chance to perform replica on the specimen one more time after determination of residual stress. In addition, depth resolution performance is not good as XRD technique in terms of comparison.

Determination of residual stress based on non-linear elastic techniques may result in misinterpretations. For instance, effect of microstructure and environment, manufacturing processes and anisotropy in the microstructure lead to remarkable deviations in the measurement results. Therefore, it is essential to compare samples with stress relieved ones that needs to be in a same physical conditions. As a result, the technique is usually not appropriate for continual residual stress measurement applications.

While measurement of residual stress, it requires at least two exactly given orientation concerning surface plane of the material to acquire formed strain on the lattice. As a result, investigated material shall be crystalline (preferentially not large grain) to evaluate residual stress. XRD generates diffractions coming from different orientation concerning surface of the specimen. Hereby, material could be ceramic or metallic for XRD and it is essential to obtain sufficient intensity by peaks and independent from adjacent peaks. The technique presents feature having replica chance due to no-destructive character of the method for verification purpose.

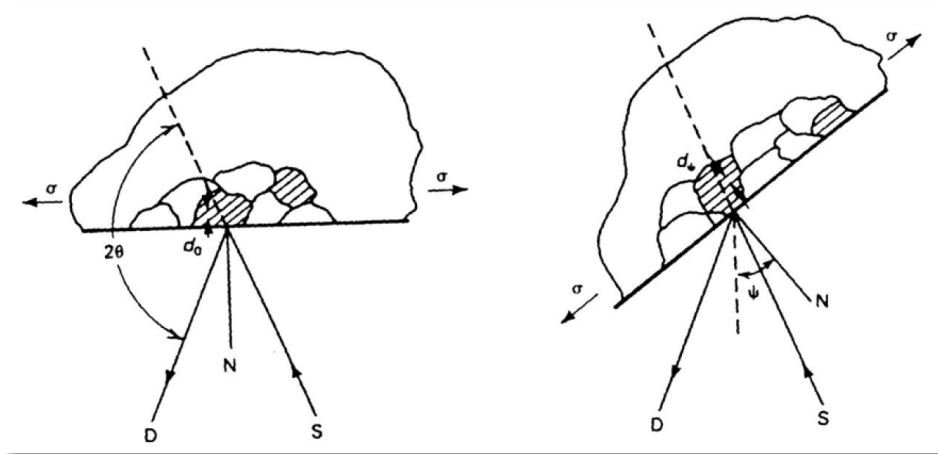


Figure 20 Given two orientations: $\psi=0$ (left) and rotation ψ angle (right) [34]

Macro scale stress is obtained from measurement in large region of microstructure (many grains) and it is evaluated in design stage and failure criteria of the picked material. The quantity of stress is evaluated according to stress tensor that alters to direction of force. For each surface on a unit cube, the stress on that surface can point in each of three directions. Particular direction and position on the surface deliver residual stress by evaluating strain in selected direction.

Stress triaxiality is a notion that picking up concerning state of stress. It generally yields the way looking at strain and therefore plastic deformation. To interpret the macro stress, three common directions and state of plain stress shall be introduced. Later, principle stresses are calculated by the help of Mohr's circle to obtain highest and lowest residual stress. Crystal lattice under loading changes their original position that leads to change in diffraction angle and resulted in formation of strain on the material.

Micro scale stress is numerical feature of the material. For instance, hardness value or amount of work hardening which doesn't depend on the location and direction can be illustrated. Their values are connected with number of defects in the microstructure. These stresses are correlated with formed strain in the transverse position of lattice. Microstresses change according to lattice spacing and broadening of the peak within the

crystal lattice. Therefore, definite location exhibits diversity due to aforementioned reasons. As a result; macro and micro scale stresses are obtained from crystal lattice spacing and broadening of the peak under separate cover.

2.6.1. BASICS OF XRD RESIDUAL STRESS EVALUATION

Monochromatic beam of X-Ray is diffracted on the surface of retained stress on specimen at a diffraction angle (2θ). Orientation of specimen surface is described by ψ angle which is degree between diffracted X-Ray beam and normal plane of surface.

X-Ray diffraction angle is described according to Bragg's Law:

$$n\lambda = 2d \sin \theta \text{ where;}$$

n : an integer (constructive interference occurs when n is an integer)

λ : the wavelength of the rays

θ : The angle between incident rays and surface of the crystal

d : Spacing between layers of the atom

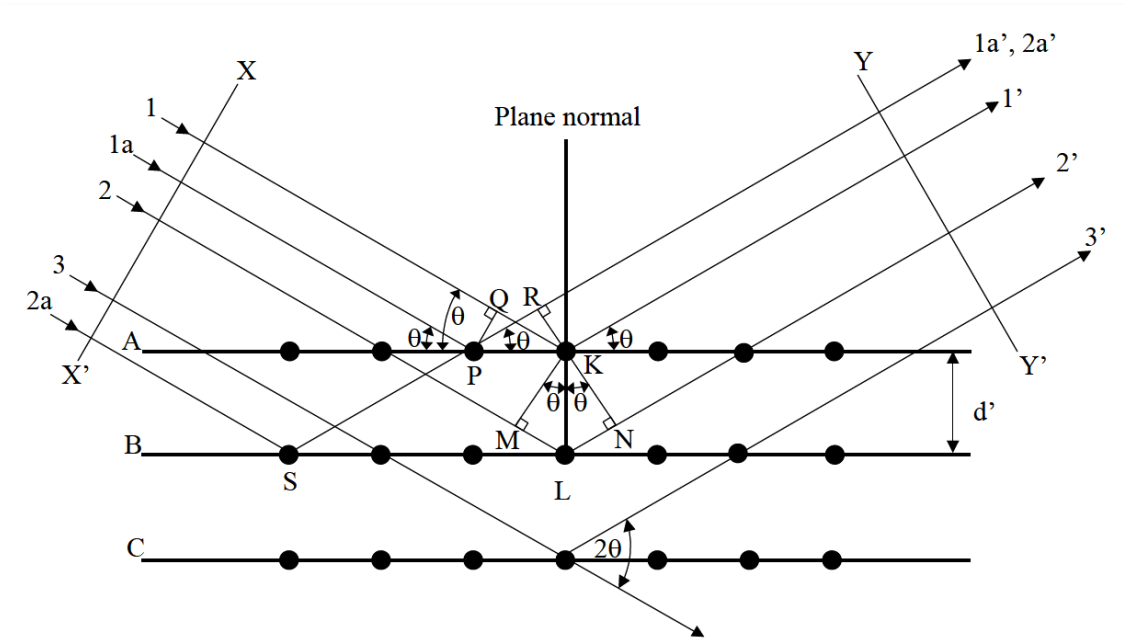


Figure 21 Constructive interference of reflected waves [35]

The wavelength is received between 1 to E+05 for the monochromatic X-Rays generated by metallic object of an X-Ray tube. Herein, diffraction angle will alter according to alternating interlaminar d spacing. Formed tensile stress on the material leads to decreasing space between layers of atoms and rising diffraction of angle in the case of $\psi = 0$ orientation. On the other hand, rotation of specimen along a define angle (ψ); interlaminar distance will increase and leading to decrease diffraction angle due to existence of tensile stress on the surface of material. Hereby, at least two measurement for each orientation will reveal the formed residual stress on the surface of the material by observing the change in diffraction angle. Specimen is rotated over its surface to evaluate retained stress in diverse directions at a single point.

Macro scale stresses measurement is based on change in elastic strain through crystal lattice by XRD method. Upon plastic strain exist under loading, crystal lattice is dispersed through dislocation motion; as a result, micro scale stress is acquired. Nevertheless, creation of plastic strain doesn't affect the macro scale stresses. All types of residual stresses associated with formed elastic strain on the microstructure are caused by permanent deformation under processing.

The basic principle of residual stress measurement through XRD technique is based on arithmetic mean of stress in definite volume of sample. Herein, the amount of residual stress alters according to target area and depth profile from surface of diffracted beam. Penetration depth of XRD beam is directly influenced by linear absorption coefficient of sample. Retained residual stress is evaluated through knowledge coming from 50 microns depth that is approximately half of the radiated beam for iron, aluminum alloys and nickels. Nevertheless, output for residual stress measurement in terms of resolution is much better than other type of techniques [18].

To evaluate residual stress on the material; certain plains are taken into consideration due to limitations of X-Ray source to generate wavelength though measurement can be performed through any spacing between layers of atom. During performing residual stress

measurement, accuracy depends on picked diffraction peak. For this purpose, diffraction angle (2θ) is usually preferred as higher than 120° . For instance, advised elastic constants for AISI 4140 steel is stated below;

Radiation is supplied by Cr $K\alpha$, lattice plane is (211) and diffraction angle is 156.0° .

X-Ray residual stress measurement is usually performed by three basic methods: single-angle, two-angle, and $\sin^2\psi$ techniques by presuming plane stress on the surface of specimen. Among them, single-angle technique is less precise one due to constrain on rotation angle by diffraction angle. Increasing diffraction angle leads to decrease in $\sin^2\psi$ for precision. Formed residual stress alters on the surface according to inter planar distance in lattice.

Another technique; in case of that inter planar distance is proportional with $\sin^2\psi$; stress is measured through two ψ orientation angle; generally $\psi=0^\circ$ and $\psi=45^\circ$. The two-angle technique provides high precision due to high diffraction angle.

$\sin^2\psi$ technique has same idea with two angle technique. Only difference is chance to have many tilts during analysis. The advance of $\sin^2\psi$ technique is to attain linearity of inter planar distance as a function of $\sin^2\psi$ during residual stress measurement although it requires extra time for data collection. The Marion-Cohen technique is preferred for extremely textural samples. Marion-Cohen, two angle technique and $\sin^2\psi$ method give approximately same output in terms of residual stress for shot peened components.

Full-tensor technique is preferred for machining or ground specimens to reveal surface stresses by analyzing Psi splitting. However, it requires additional data collection and unstressed lattice spacing to acquire sensitive strain data for residual stress measurement.

2.6.2. RESIDUAL STRESS MEASUREMENT TECHNIQUE

Before starting residual stress measurement, sample preparation is required to be compatible with X-ray source and its dimensions are usually specified as small. Sample preparation method alters according to purpose of application. For example, machined

surface shall be avoided from corrosion or etching not to affect formed residual stress zone. Therefore, some protective abrasives like Molykote can be used to prevent formation of additional stress on the surface of material. On the other hand, secondary treatment after machining like abrasive treatment creates compressive zone on the surface. Eletropolishing is recommended any type of heat treatment operation. As a result, surface is eliminated from retained stresses and focused on subsurface by the help of eletropolishing.

Sample positioning is also critical in terms of providing precision. Specimen shall be mounted in X-Ray beam to enable orientation and diffraction angle. During radiation, orientation shall be kept stable. Geometry of the specimen affects the uncertainty on residual stress measurement. Flat dimensions yield less error; on the other hand, round surfaces result in higher uncertainty. Therefore, all these considerations shall be evaluated before measurement to get reliable output.

Before starting measurement, X-Ray beam size shall be judged since residual stress evaluation is basically affected by dimension of the beam. It depends on the purpose of application. For instance, small beam size can be preferred in case of local measurement to reveal alteration in residual stress. On the other hand, large beam size is like better upon the target is to observe large area to find out mean stress. In case of focusing large area to collect data; required measurement time will decrease. It is correlated number of diffracted beams to get reliable intensity from XRD measurement since it is proportional with number of diffracted beams. To obtain higher accuracy; high number of diffracted beam is required without considering time. In case of decreasing radiated zone, it leads to decreasing intensity precision and measurement time.

X-Ray is produced from metal target to attain residual stress measurement. The target metal generates white radiation and three monochromatic peaks. Three intensity lines are $K_{\alpha 1}$, $K_{\alpha 2}$, and K_{β} and they are used to obtain sensitive output. Among them, $K_{\alpha 1}$ is the highest one, then $K_{\alpha 2}$, and K_{β} respectively. K_{β} is undersized one and not preferred for the

XRD residual stress measurement. Usually, $K\alpha$ is used to evaluate residual stress retained on the plastically deformed material.

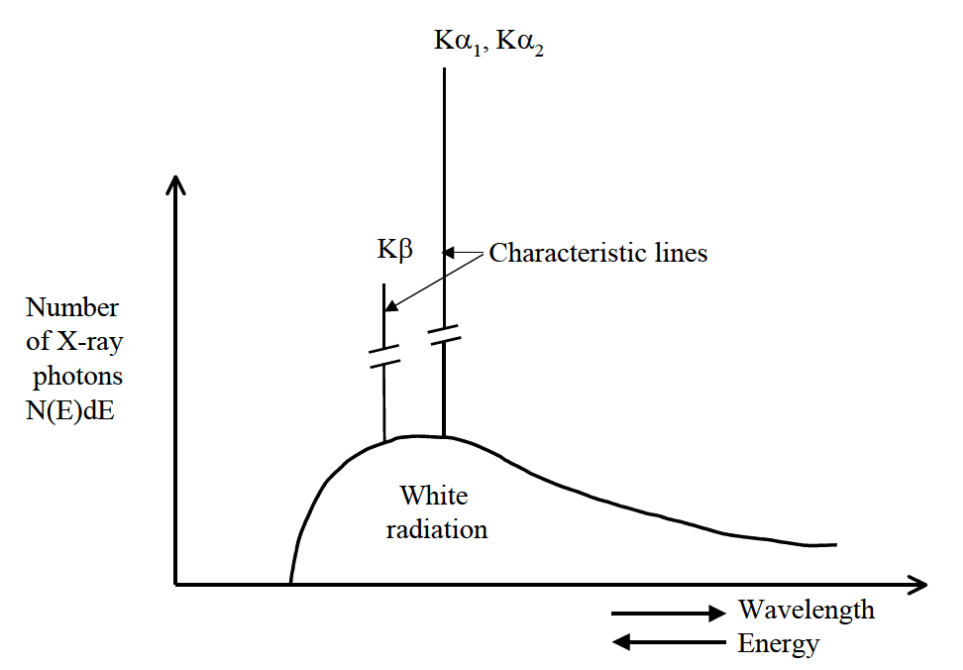


Figure 22 A typical spectrum of emitted X-Rays from an X-Ray tube [35]

Herein, broad peaks are critical during determination of residual stress since it is related with the precision of diffraction. Sharp peaks have less precision rather than broad peaks. As a result, precision of diffraction is connected to collected number of x-rays that requires more time and broaden peaks.

Acquired intensities need to be modified by the help of Lorentz polarization and absorption prior to peak position. Then obtained intensity is subtracted from background intensity through presuming linear elastic distortion of lattice. Every resulted technique of peak location can induce some errors due to variation in doublet difference.

The reasons behind of diffraction peak broadening are because of formed residual stresses in the lattice and crystal size. Herein, dissociation of broadening because of straining and

crystal size are carried out FTT method. Eventually, it describes diffraction-peak plot by evaluating adequate data. It requires excessive data for broadening separation.

Fluorescence problem exists for specimens during performing residual stress measurement. The desired purpose for radiation is to obtain highest precision. Generally, Cu K_{α} radiation is preferred for residual stress measurement in alloys containing Fe, Cr and Ti elements. Eventually, fluorescence background forms as high as diffraction and leads to formation of noise. Some solutions can be considered such as usage of metal foil filter. Nevertheless, it results in deterioration of precision by increasing errors in the analysis. As an alternative; monochromators and solid state detectors can be operated. Those detectors present inefficient energy resolution to surmount fluorescence during residual stress measurement.

2.6.3. SOURCES OF UNCERTAINTIES

While performing residual stress measurement, peak positioning may result in severe amount of deviation in the stress. For instance, errors of 10 microns in the positioning lead to underestimation of the residual stress. Therefore, alignment is critical before analysis and involves coincidence of diffraction angle and orientation angle. Therefore, diffracted body needs to be positioned to the axis of rotation and diffraction angle. After ensuring alignment of the sample, alignment of diffraction instrument shall be checked to prevent presence of errors on the result of measurement.

Surface condition of the specimens also affect the reliability of results. For example, roughness, pitting corrosion, geometry directly etc. influence the error level. Besides, particularly the cast components having large-size grains resulted in less number of diffraction peaks with a non-proportional character. In addition, X-Ray elastic constant shall be obtained empirically to minimize error since it exhibits elastic anisotropy.

CHAPTER 3

LITERATURE REVIEW

This section presents the literature review about effect of shot peening on fatigue life and measurement of residual stress in shot-peened components.

Hozapfel et al. (1996) investigated the effect of shot peening parameters: peening pressure, hardness of workpiece and shot media, mass flow rate and size of shot media for AISI 4140 steels. The compressive stresses were evaluated by the help of XRD (*Figure 23*). Accordingly, increasing workpiece hardness decreased the skin depth; nevertheless, it increased the amount of compressive residual stress. In addition, increasing mass flow and peening pressure led to increasing compressive residual stresses [16].

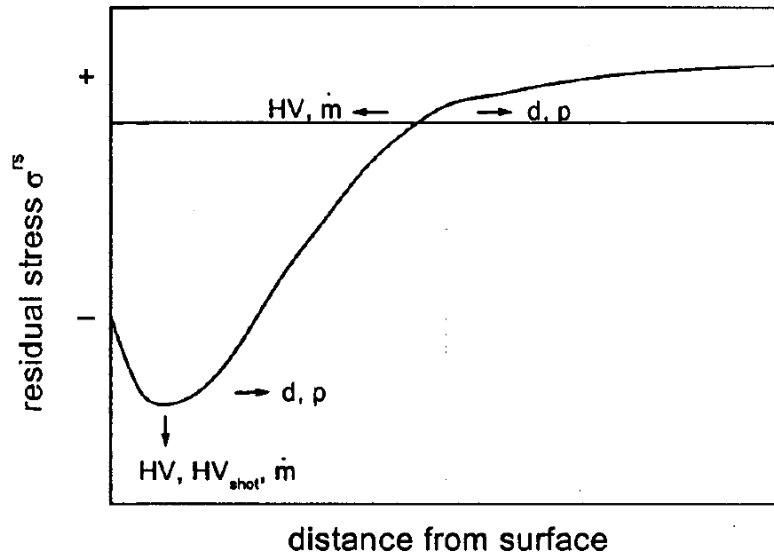


Figure 23 Depth profile of residual stress in shot-peened AISI 4140 steel [16]

Monin et al. (2000) studied inhomogeneous residual stress state and surface roughness caused by shot-peening. XRD stress measurements were performed according to the $\sin^2\psi$ -method at the top and bottom of a Brinell indentation and measurements were obtained at a distance of 0,2 mm, 1 mm, 2,5 mm and 5 mm from the mark side. Consequently, inhomogeneous residual stress distribution through tops of the indentation was discovered in terms of different magnitude and sign and various indentations do not take off the inhomogeneity of residual stress state.

Palma et al. (2003) obtained a relationship between MBN RMS values and fatigue cyclic number. MBN value increased by increasing amplitude of stress which also creates microstructural change in the material. They clarified that resistance to the movement of slip mechanisms due to cyclic loading makes the movement of domain walls more difficult. They displayed that MBN value reduces on the high cycle region because of aforementioned reason.

Lopes et al. (2008) studied fatigue limit of AISI 4140 steel for different feeding rate, depths of cut, cutting speeds in machined condition. Tests were performed at room temperature with cyclic frequency of 58 Hz on rotating bending fatigue testing machine. Mean stress was determined as zero before testing and tests were carried out according to stair-case methodology as shown in *Figure 24* to predict fatigue limit. Test type was chosen as constant amplitude bending moment. They presented changes of endurance limit machining parameters. Eventually, they reported that the polished specimen without stress relief heat treatment had the highest fatigue limit.

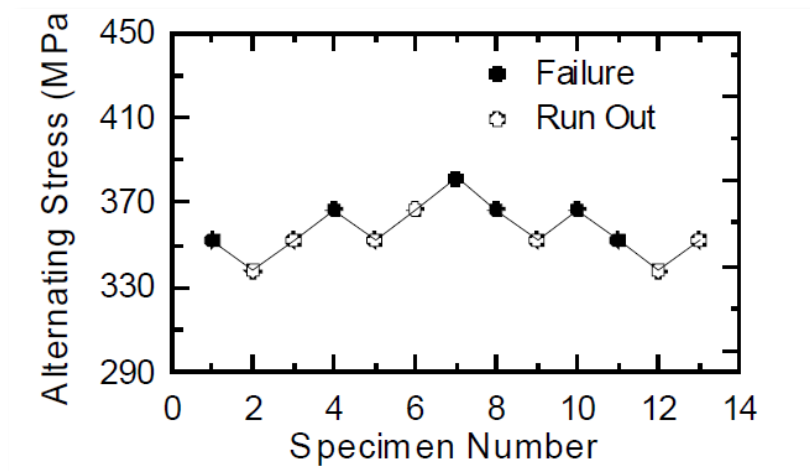


Figure 24 Stair case method to determine fatigue life [2]

Lammi (2009) studied the effects of residual stresses on fatigue crack growth via optical and scanning electron microscopy. He concluded that residual stresses influence the crack growth rate and also crack propagation path. The samples having lower residual stress came out fracture surfaces with lower branching [41].

Savaş et al. (2010) studied non-destructive measurement of surface residual stresses in the shot-peened steel specimens by MBN technique. The MBN evaluation displayed that MBN signal distinctly differs depending on shot peening parameters. They verified residual stress measurement by XRD method. They concluded that peening process forms significant amount of compressive residual stress in the surface region of specimens and

the residual stress increases by shot severity, coverage and nozzle angle. Differently my contribution was to verify residual stresses measurement by fatigue testing under constant amplitude load control besides non-destructive methods [9].

Alang et al. (2011) studied the influence of surface roughness on fatigue life of steels having artificial defect. The fatigue tests were performed on a cantilever rotating bending testing machine with 50 Hz cyclic frequency at $R=-1$ stress ratio. Fracture surfaces were investigated by SEM and optical microscopy. They observed that lower surface roughness enhances the fatigue life in the high cycle region; however, no substantial improvement exists in the low cycle region (*Figure 25*); and crack initiation sites were created in the samples having coarser surface finish [17].

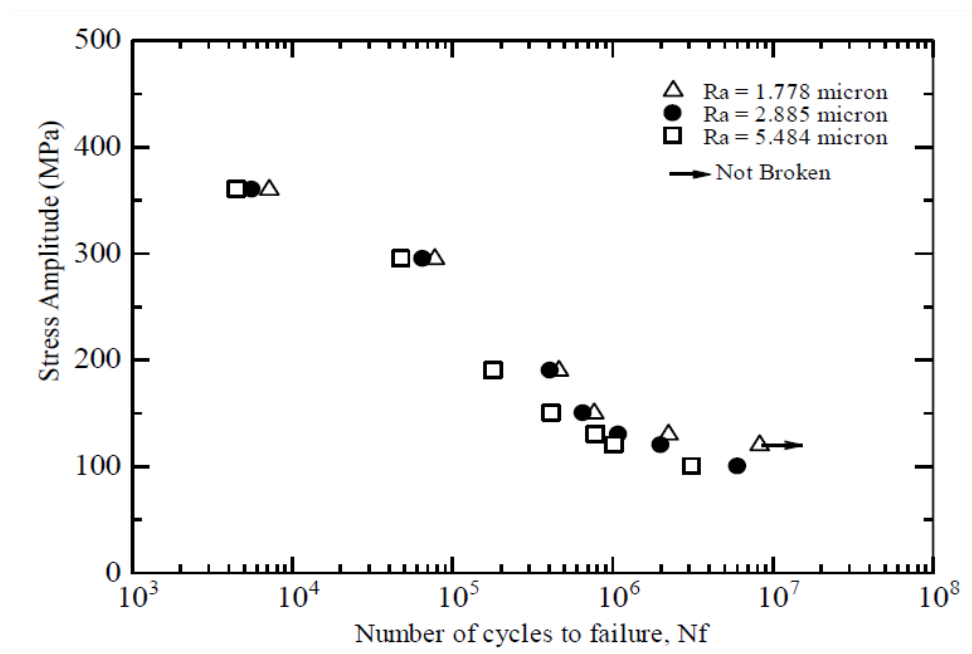


Figure 25 Effect of surface roughness on fatigue life [17]

Lundberg et al. (2013) studied influence of shot size, coverage and shot intensity on residual stress in flake and vermicular cast irons. Measurements by XRD method gave compressive residual stresses in the range of 245 to 565 MPa. Eventually, the highest

compressive residual stress was belonged to the sample peened at the lowest shot intensity, size and coverage (*Figure 26*). They also reported that increased shot severity remarkably influences the depth profile of residual stress [1].

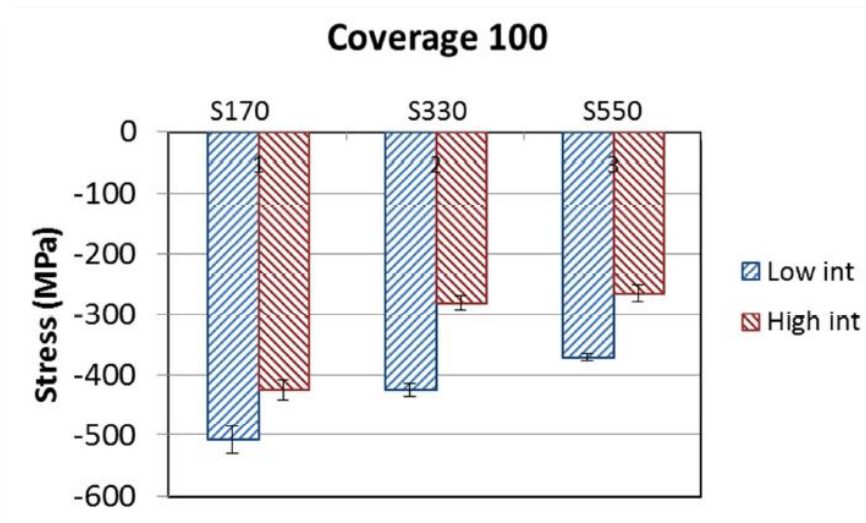


Figure 26 Effect of shot media parameter on the magnitude of compressive residual stress [1]

Buttle et al. (2013) overviewed on the multi-parameter MAPS (Magnetic Anisotropy and Permeability System) method and the MBN method to reveal residual stresses in the microstructure. According to this paper, as a result of the MBN signal as electromagnetic diminution, the skin-depth procurement of the MBN signal is hedged to the near-surface region of approximately less than 1mm, but this fact strenuously is bound up with the magnetic excitation frequency and permeability of the material.

Žerovnik et al. (2014) stated that magnitude of the residual stress varies with skin depth of the component and maximum value of the residual stress is determined by stress versus skin depth graph in shot peening case. They measured compressive residual stress in the surface region of material by the help of Magnetic Barkhausen Noise technique. Additionally, they verified residual stress measurement by blind hole drilling. They concluded that the lowest air pressure and the lowest peening time lead to the lowest

surface roughness. By performing equal period of shot peening, the surface roughness of the sample was improved for higher pressure condition. Another result was that holding longer times led to rougher surface roughness.

CHAPTER 4

EXPERIMENTAL PROCEDURE

4.1. MATERIAL

AISI 4140 steel (0.40%C, 0.25%Si, 0.85%Mn, 1.0%Cr, and 0.25%Mo in weight) was selected for the experiments.

4.2. SAMPLE PREPARATION

The fatigue test samples (*Figure 27*) were prepared according to ASTM E466 standard by using the parameters given in *Table 1*. Totally 25 specimens were manufactured during experiments. Sample form was determined as longitudinal before manufacturing. Stress relief heat treatment was applied at 800 °C for 2 hours and then furnace cooled. After metallographic sample preparation, micrographs were obtained via optical microscope. To determine optimum magnetization and amplification values of the MBN equipment, calibration was performed using the initial not-peened specimen.

Table 1 Machining parameters of the AISI 4140 steel samples

Rough Machining		Finishing	
Feed Rate (mm/rev)	Cutting Speed (rev/min)	Feed Rate (mm/rev)	Cutting Speed (rev/min)
0.18	850	0.02	850

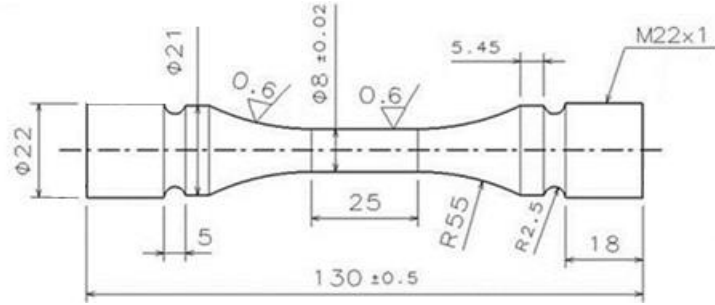


Figure 27 Drawing of the fatigue test specimen [37]

4.3. SHOT PEENING PARAMETERS

Shot peening operation requires precision and repeatability. These requirements are met by privileged and fully-automatic process control system. In this study, NADCAP certified conventional air pressured shot peening equipment at Turkish Aerospace Industry, Inc. was used.



Figure 28 Shot peening equipment (TAI)

Three different intensities (3-6, 4-7, 6-10 Almen) and two coverage percentages (200% and 300%) were selected as test variables. The chemical composition of the shot media

was 1.0%C, 0.84%Si, 0.97%Mn, 0.018%S, and 0.019% P. Ten hardness measurements were performed for hardness and average value was found as 45.3 HRC. Density of shot media was 7.0 gr/cm³. Any defects like voids, shrinks and cracks on shot media were not observed before shot peening process.

Shot peening processes were performed manually to obtain three different intensities. Certain intensity ranges were preferred to ensure the intended intensity rather than precise value. For instance, 3A-6A was determined as severity parameter. In order to convert Almen intensity to the SAE standard; it shall be multiplied by 40. As a result; 6A corresponds to 0.15 mm Almen intensity.

Shot penning operation was performed manually by identifying shot mass flow rate as 8000 g/min and air pressures as 800mbar or 1000mbar depending on shot-peening parameter. The required time was separately measured from cross sectional area of the samples and also for Almen strip during shot-peening and their results are tabulated in *Table 2*. Almen strips shown in *Figure 29* were used to control shot-peening by measuring shot intensity. Almen strip time (t_{st}) is calculated using equation 4.1;

$$t_{st} = \frac{A_{sp} \times t_{sp}}{A_{st}} \quad (4.1)$$

t_{sp} : Processing time, A_{st} : Cross sectional area of the Almen strip, A_{sp} : Cross sectional area of the specimen.

Table 2 Almen Strip Results

Sample Code	Intensity	Coverage (%)	Almen-Time (seconds)	Pressure (mbar)	Value	Process time (sec)
-	3A-6A	100	17.3	800	0.0046	-
3,5,19		200	34.6	800	0.0058	1' 10"
12,17,20		300	69.2	800	0.006	2' 20"
-	4A-7A	100	12	800	0.0053	-
7,14,18		200	24	800	0.0056	1'
1,11,23		300	48	800	0.006	2'
-	6A-10A	100	7.5	1000	0.006	-
9,13,15		200	15	1000	0.0067	47"
10,21,24		300	30	1000	0.0073	1' 34"

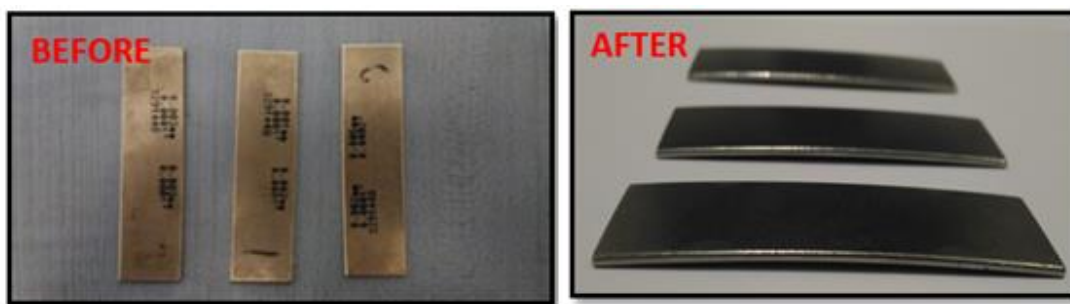


Figure 29 Deflection of Almen strip

4.4. SURFACE ROUGHNESS MEASUREMENT

After shot-peening; surface roughness values were measured to ensure that all samples approximately have the same roughness value. The purpose was to eliminate the effect of surface roughness on fatigue life by demonstrating close Ra values for each specimen. A surface evaluation system (Mitutoyo) was used in the surface roughness measurements. Surface roughness was evaluated by using the arithmetic mean value (Ra), the Root Mean Square (Rq), and the vertical distance from the highest peak to the lowest valley within

five sampling lengths (Rz) over the gauge length of the samples. The surface roughness measurements on each specimen were replicated three times to boost reliability of the data. The average values and standard deviations were calculated and tabulated in *Table 3*. In addition, the scatter of data is shown in *Figure 30*.

Table 3 Surface roughness parameter values

Sample Code	Coverage (%)	Intensity	Ra (μm)	Rq (μm)	Rz (μm)	Rmax (μm)
SP3	200	3A-6A	1.161	1.439	5.026	6.566
SP5			1.309	1.645	6.122	7.805
SP19			1.181	1.486	5.558	7.291
SP12	300	3A-6A	1.153	1.41	5.141	5.945
SP17			1.507	1.851	6.956	8.622
SP20			1.056	1.269	4.605	5.614
SP7	200	4A-7A	1.225	1.531	5.314	7.133
SP14			0.975	1.247	4.488	6.207
SP18			1.225	1.519	6.05	7.265
SP1	300	4A-7A	1.204	1.488	5.859	7.962
SP11			1.124	1.391	4.861	5.986
SP23			1.337	1.685	6.074	8.132
SP9	200	6A-10A	1.663	2.064	7.347	9.290
SP13			1.505	1.834	6.221	8.418
SP15			1.408	1.752	6.541	8.256
SP10	300	6A-10A	1.527	1.929	6.796	10.226
SP21			1.484	1.845	6.698	9.266
SP24			1.659	2.031	6.696	8.826
Average			1.317	1.634	5.908	7.712
Standard Deviation			0,204	0,251	0,856	1,309

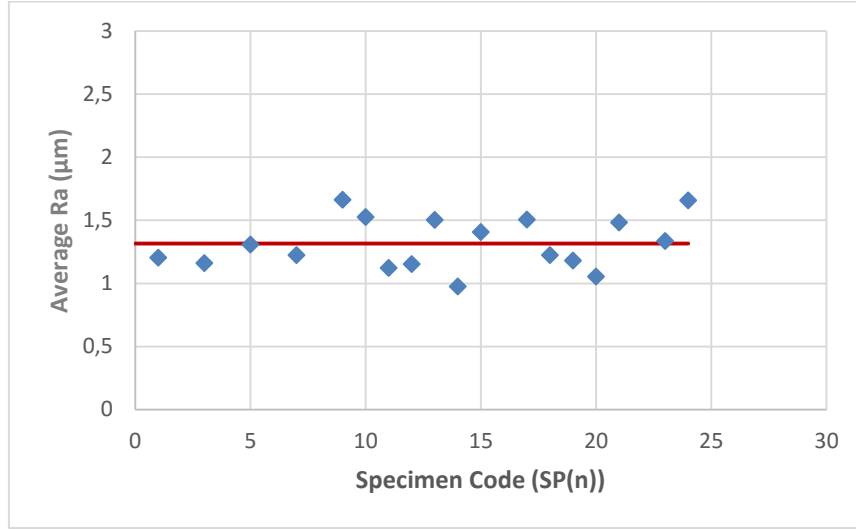


Figure 30 Scatter of surface roughness

4.5. RESONANT FATIGUE TESTING

Fatigue tests were performed at room temperature on an axial resonant testing machine (RUMUL Testronic in TAI Inc.) executing a cyclical frequency of approximately 140 Hz and a stress ratio of $R=0,1$ i.e., tensile-tensile cyclic loading.

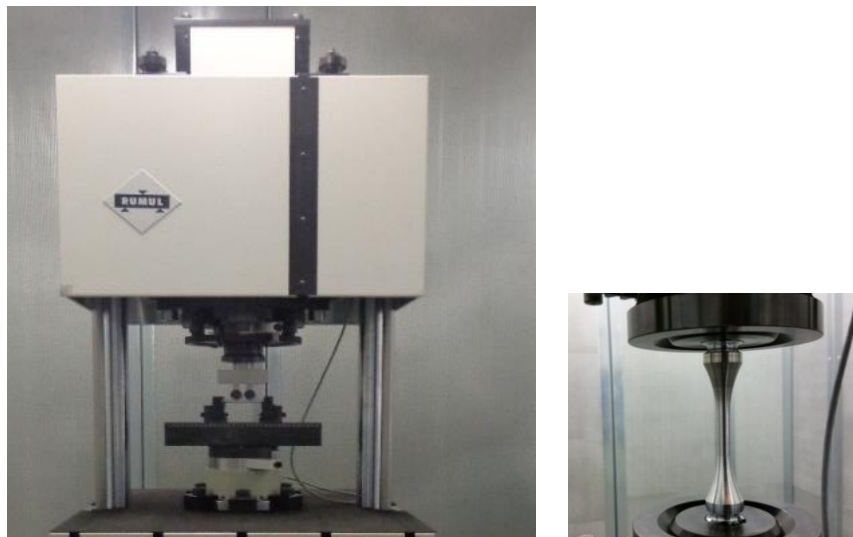


Figure 31 Rumul resonant fatigue machine (TAI M&P Lab.)

The load cell of system was 100 kN capability. All the tests were performed under load control condition. Mean and amplitude of the load were kept constant during testing. Alignment of the testing device was certified to be lower than 5 % maximum bending according to ASTM E1012 and calibrated per Class-1 of ISO7500-1. The testing environment was set as constant temperature of 25 ± 3 °C and 50 ± 5 RH during the test. All specimens were mounted to the resonant fatigue machine that appointed as cyclic loading system.

4.6. MAGNETIC BARKHAUSEN NOISE MEASUREMENT

MBN measurements were performed using Stresstech 500-2 equipment. Electromagnetic field leads to domain wall movement inside the material. The measurement depth depends on frequency, conductivity and permeability of the analyzed material. For practical applications, measurement depth alters between 0.01 and 1.5 mm.

The equipment easily detects defects caused by microstructural change. The machine also controls the surface quality for ferromagnetic materials.



Figure 32 Stresstech MBN System (METU Central Lab.)

The MBN equipment basically contains two channels, namely roll-scan and μ -scan. Roll-scan presents real time measurement and evaluates magneto-elastic parameter value; whereas, μ -scan assures the offline measurement that enables to possess the plot of pulse

height distribution and hysteresis curve of measured material. A cyclic magnetic field was induced in a small part of the sample by the help of a coil, sparked with alternating current.

The samples were magnetized by an amplified alternating current through the wire coiled up straightly on the test sample. The longitudinal axis of the sample was chosen as the measurement of MBN due to axial fatigue test. MBN measurements were carried out unloaded state and under compressive loading to reveal residual stress. Hereby, the excitation frequency was 125 Hz and the MBN measurements were performed by using the sensor, S1-138-13-01. Barkhausen signals were analyzed between 20 to 1000 kHz frequency range that was determined based on electromagnetic skin depth calculation. The proper contact of the sensor was assured to apply the same contact pressure on each specimen.

4.7. CALIBRATION

Three specimens were chosen for calibration. First specimen was used to determine the optimum measurement parameters under 125 Hz excitation frequency. After repeating the measurements for various combinations 30 A/m Magnetization and 30 A_m Amplification were chosen as the optimum calibration parameters. Then, measurements were performed on the other specimens for the optimum condition to find the specimen having the least deviation and the highest reliability. Totally 12 measurements were performed by 30° intervals on the surface, and the results are given in *Figure 33*.

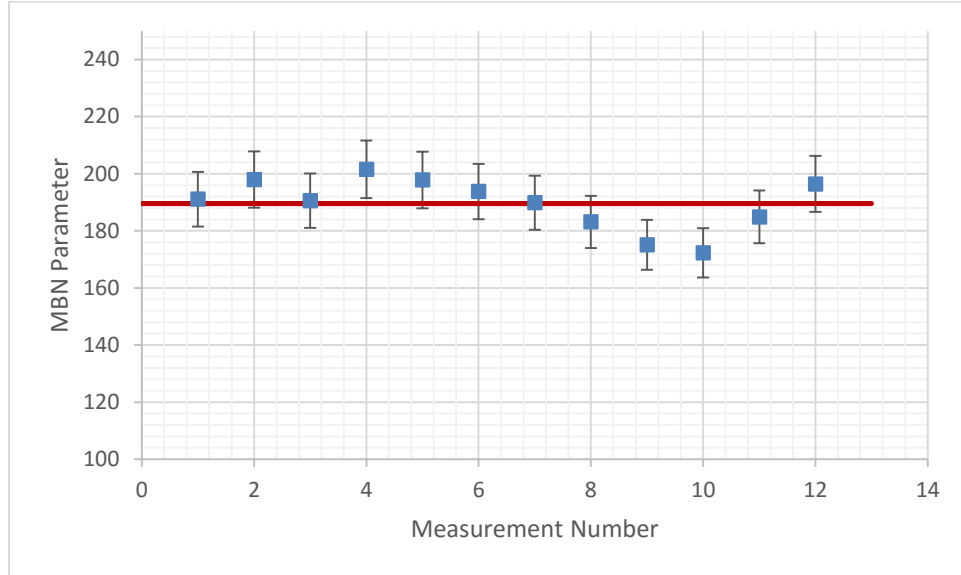


Figure 33 Scatter of MBN parameter (Roll-Scan Measurements)

The samples were incrementally loaded to create compressive stress by using Zwick electro-mechanic testing machine at METU central Lab. Reference sample was loaded until 10 kN and MBN values were recorded during loading. MBN value started to decrease by progressively loading. The resulted data can be seen in *Figure 34*.

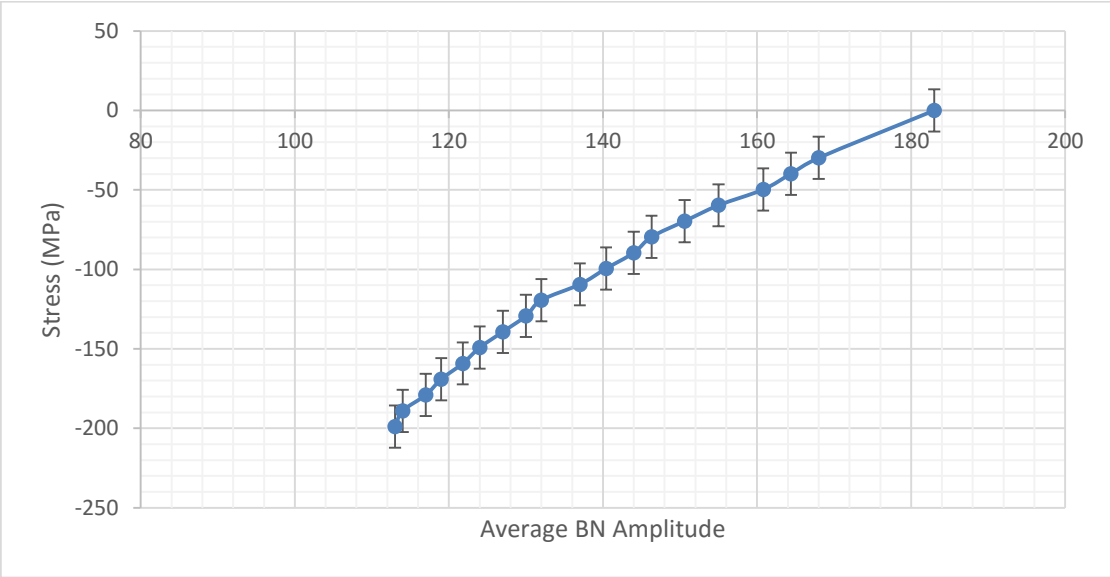


Figure 34 Calibration curve (initial sample)

After calibration of the specimen in terms of MBN; totally 18 specimens were shot peened based on aforementioned parameters.

MBN measurements can be carried out by operating a low magnetic excitation frequency that is in the range of 0.1Hz to 1Hz with the frequency range of 0.5 to 100 kHz to analyze of the MBN signal. Another option is to perform the measurement by operating a high magnetic excitation frequency which is in the range of 10 to 125 Hz with the frequency range of 10 to 1000 kHz. In the industry; MBN measurement apparatus generally exerts by the high frequency excitation at 125 Hz and analysis in the range of 70-200 kHz. Hereby, the excitation frequency was set as 125 Hz. Then, magnetization and amplification values were determined as 30 by the help of reference sample. To determine frequency range, skin depth range shall be calculated. The electromagnetic skin depth δ can be calculated using equation 5.1;

$$\delta = \frac{1}{\sqrt{\pi f \sigma \mu_0 \mu_r}} \quad (5.1)$$

where;

f : Frequency, σ : conductivity, μ_0 : permeability of vacuum, μ_r : relative permeability of material.

Conductivity and relative permeability of the material are calculated by using equation 5.2 and 5.3;

$$\sigma = \frac{l}{A * R} \quad (5.2)$$

$$\mu_r = \frac{\mu}{\mu_0} \quad (5.3)$$

where;

R : Electrical resistance of material, l : Length, A : Cross sectional area

For electrical conductivity measurement (*Figure 35*), the specimen having the diameter of $\varnothing 3.2$ mm, and length of 50 mm was used. Electrical resistance was taken as 0.001Ω . As a result; electrical conductivity of the material was found as $6.22 * 10^6 \Omega^{-1} \text{ m}^{-1}$.



Figure 35 Nanovolt, Micro Ohm Meter (METU Central Lab.)

To procure relative permeability of AISI 4140, toroidal inductance that is used in pulsed power and power conditioning was measured on AGILANT 4294A (*Figure 36*). In order

to measure a magnetic core as a form to wind toroid, the inductance of toroid is calculated using equation 5.4. As a result, inductance was measured as 158 μH .

$$L \cong 0.01257N^2(R - \sqrt{R^2 - a^2}) \quad (5.4)$$

where,

L : Inductance (μH), N : number of turns, R : mean radius of the form (in cm), a : radius of the winding (in cm) on the form as shown in *Figure 37*.



Figure 36 Precision Impedance Analyzer (METU Central Lab.)

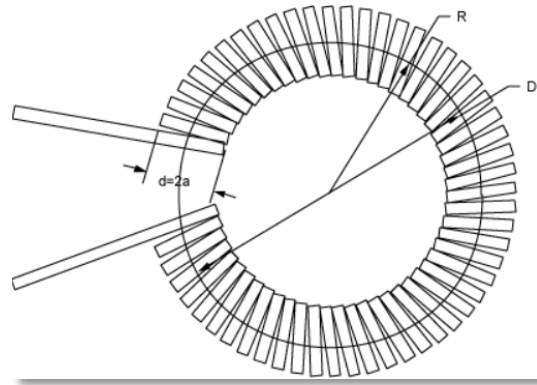


Figure 37 Diagram of a circular cross sectional toroid inductor [36]

The basic relationship between inductance and relative permeability is given in equation 5.5;

$$L = 2N^2\mu_r h \ln\left(\frac{d_1}{d_2}\right) \quad (5.5)$$

where,

L : inductance of coil in nH, N : number of turns in wire coil, μ_r : Relative permeability, h : core width, d_1 : Outer Diameter, d_2 : Inner Diameter.

The low field relative permeability of AISI 4140 steel was calculated as 46.52. The typical values of the skin depth of the MBN signal for different ranges was calculated (*Table 4*).

Table 4 Frequency ranges and corresponding skin depth values

Analyzing frequency range (kHz)	Skin depth range (μm)
1-2	935-660
2-3	660-540
3-4	540-465
4-5	420-330
5-8	330-295
10-20	295-210
20-1000	210-30

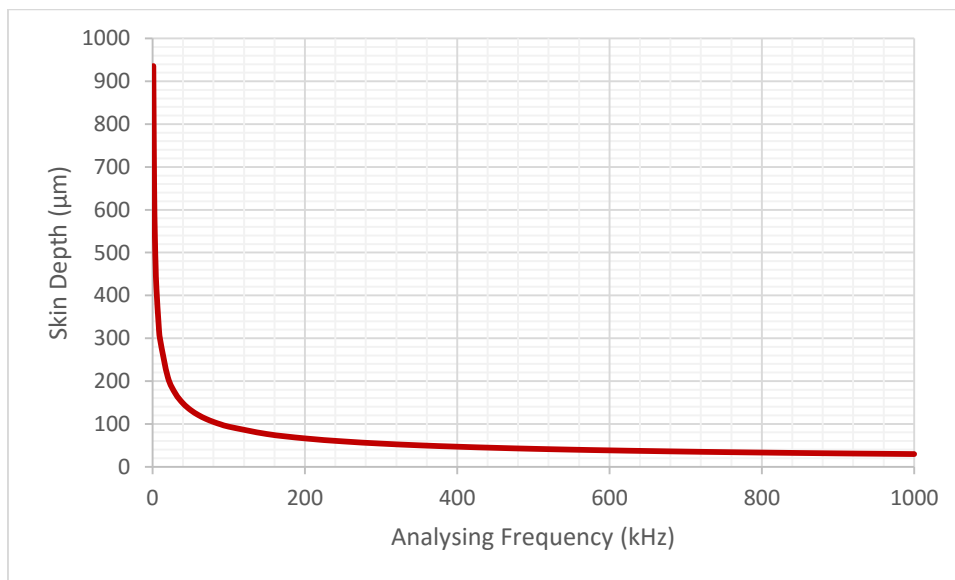


Figure 38 Change of the skin depth with frequency

Analyzing frequency range which was determined as 20-1000 kHz for high excitation frequency to pick up the MBN signal on the surface of the component corresponded to 210-30 μm skin depth range.

CHAPTER 5

RESULTS AND DISCUSSIONS

5.1. MICROSTRUCTURE OF THE SAMPLE

The microstructure of AISI 4140 steel is comprised of ferrite and pearlite with an average hardness of 36 HRC (*Figure 39*). The average grain size of the samples is $36.3 \pm 13.2 \mu\text{m}$.

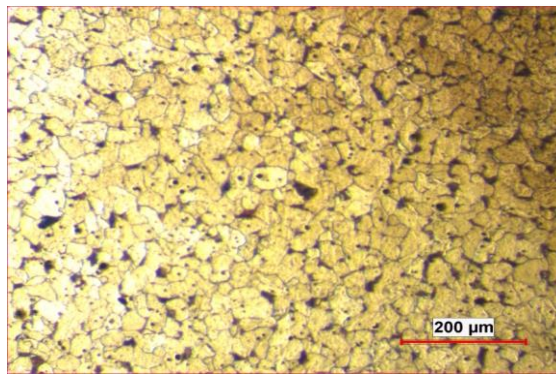


Figure 39 Representative micrograph of the samples

5.2. RESULTS OF MAGNETIC BARKHAUSEN NOISE MEASUREMENT

A number of convenient sense should take into consideration before the Magnetic Barkhausen measurements. Primarily it is shall be seized how the knowledge is to be evaluated during measurement and it should be recovered the stress distributions on the magnetized material. The present knowledge will impress which locations is more critical to take measurement, the selection of appropriate probes, and which measurement properties should be considered to acquire optimum measurement results.

The average MBN r.m.s. profiles was calculated taking at least four measurements by the help of μ -scan that acquires outputs by performing Fast Fourier Transformation. By FFT, time domain data is converted to frequency domain data to obtain MBN emission. Hereby, it is critical that a proper sensor contact shall be assuring by clips to secure the same contact pressure to each sample. By comparing the result; it shall be revealed that decreasing intensity and coverage enables enhancement in MBN r.m.s value due to forming diverse compressive residual stress for the given parameters except for 4A-7A %300 parameter case. Similar results were found by Lundberg et al. (2013), who observed the effect of shot size on residual stress instead of intensity and coverage.

To evaluate the homogeneity of the results, MBN measurement was performed under roll-scan that has real time measurement capability. Hereby, identical magnetization, amplification and excitation data were handled as μ scan case.

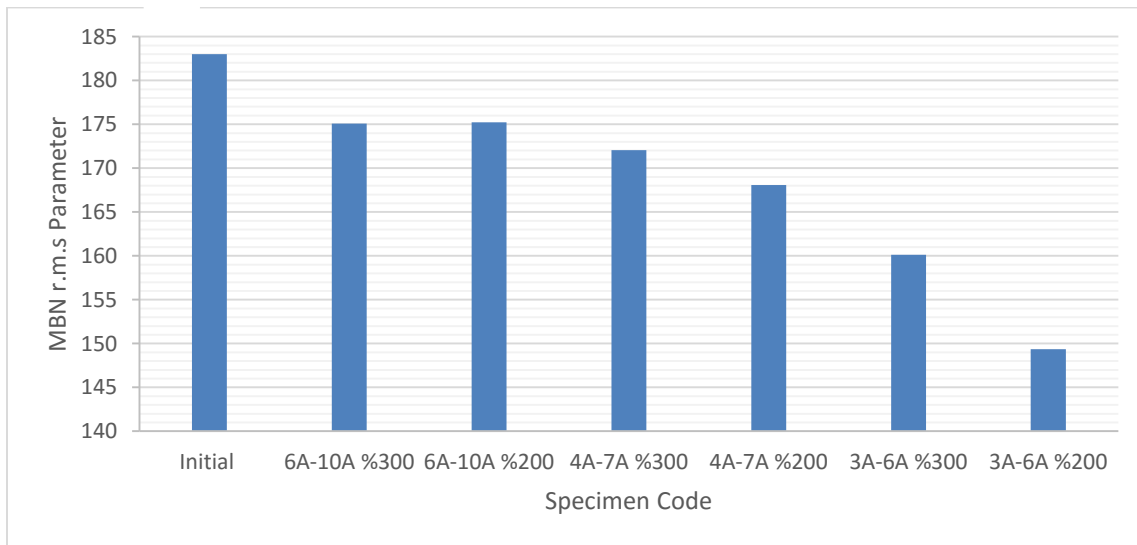


Figure 40 Variation of MBN r.m.s. value with the severity of shot peening

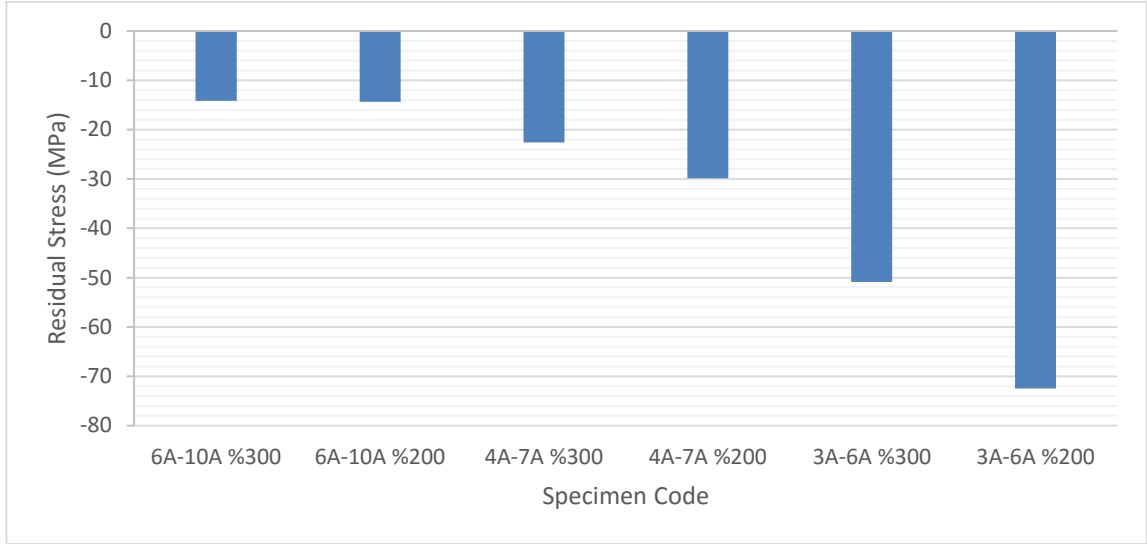


Figure 41 Variation of surface residual stress with shot-peening parameters (determined from MBN measurements)

Accordingly; -72 MPa compressive residual stress was formed for %200 coverage and 3A-6A intensity case. As a result, it can be concluded that MBN emission of AISI 4140 steel increased by decreasing intensity and coverage for aforementioned shot-peening parameters.

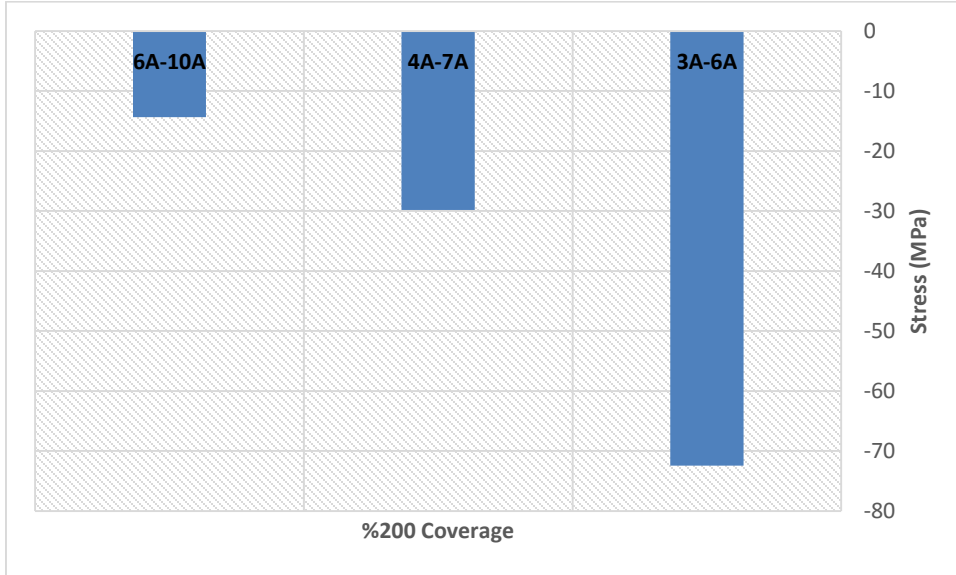


Figure 42 Variation of surface residual stress with Almen intensity (%200 coverage)

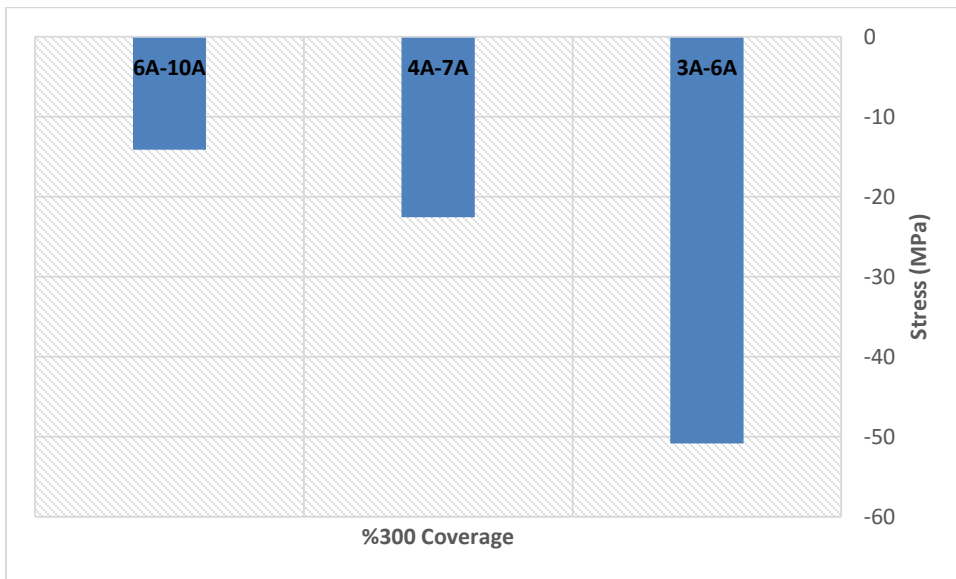


Figure 43 Variation of surface residual stress with Almen intensity (%300 coverage)

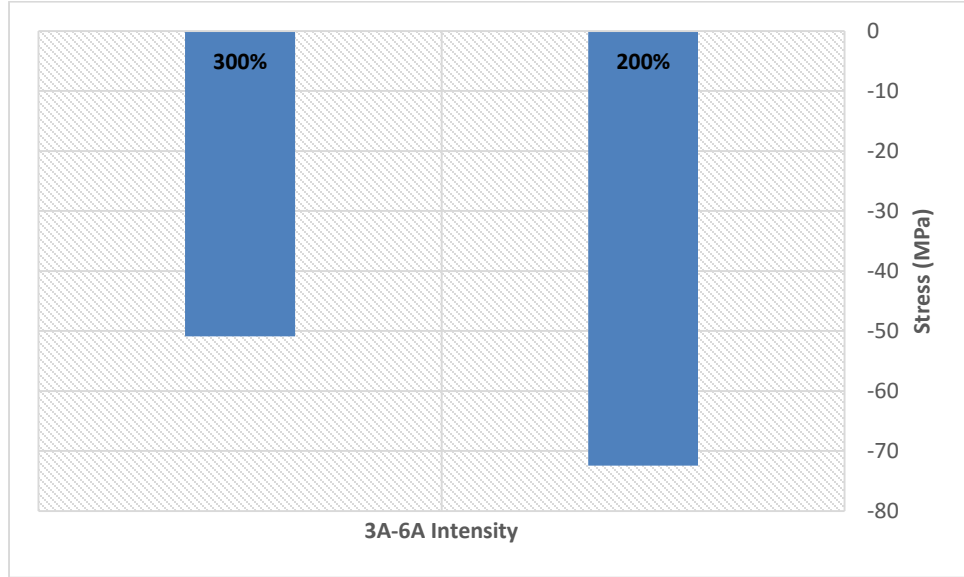


Figure 44 Variation of surface residual stress with coverage (3A-6A intensity)

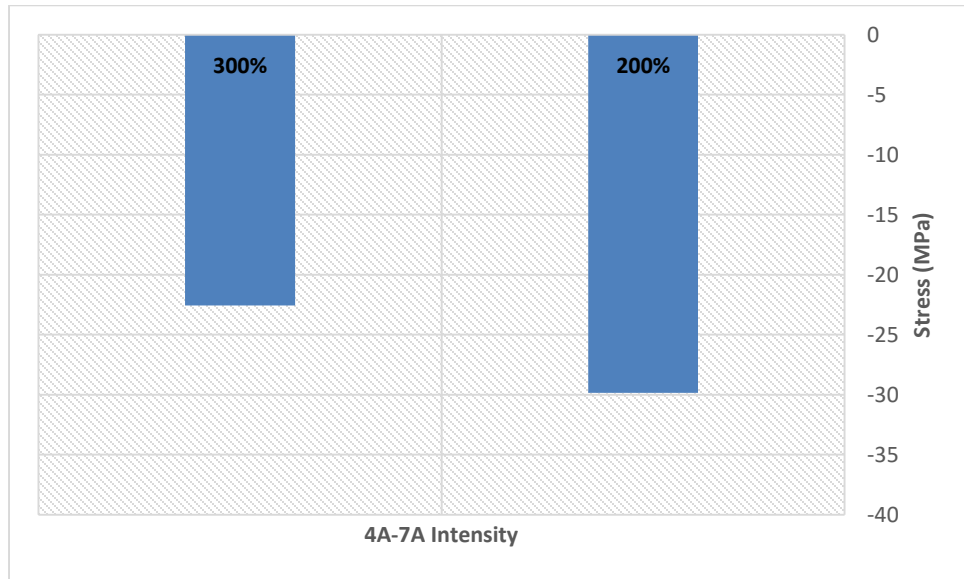


Figure 45 Variation of surface residual stress with coverage (4A-7A intensity)

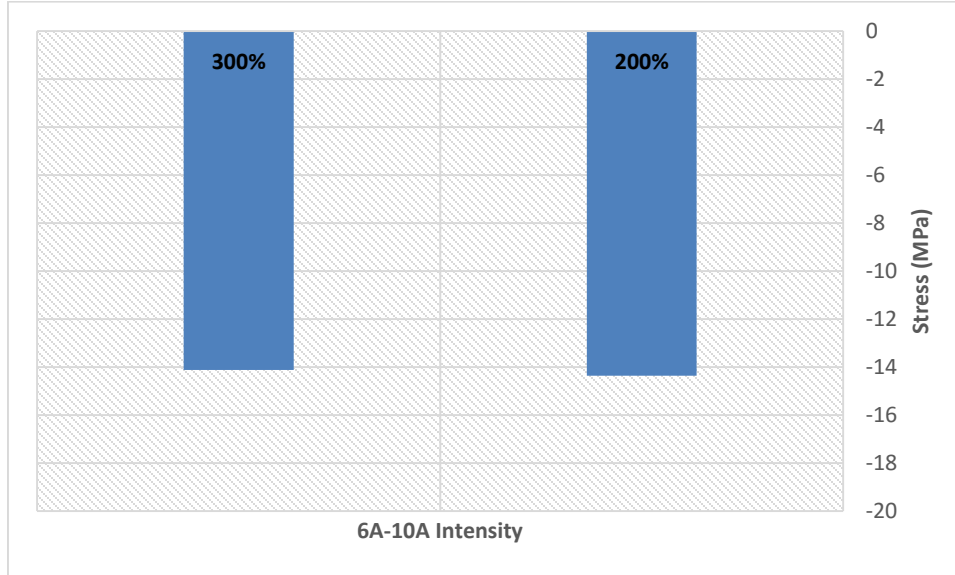


Figure 46 Variation of surface residual stress with coverage (6A-10A intensity)

Representative hysteresis curves were plotted to exhibit difference between shot-peened and initial specimens in terms of residual stress. Compressive residual stress created decrease in Barkhausen noise signal amplitude. Formed residual stresses on microstructure resulted in increasing strain and ultimately formation of smaller grains. When magnetic field is applied on the specimen, magnetic field coerces domain for magnetization to turn in its applied direction by minimizing their energy. This fact results in decreasing remanence and coercivity. Accordingly, increasing compressive residual stress on the material precisely resulted in decrease on coercivity and remanence [39]. The effect of shot peening on hysteresis curve was shown in *Figure 47* and *Figure 48*.

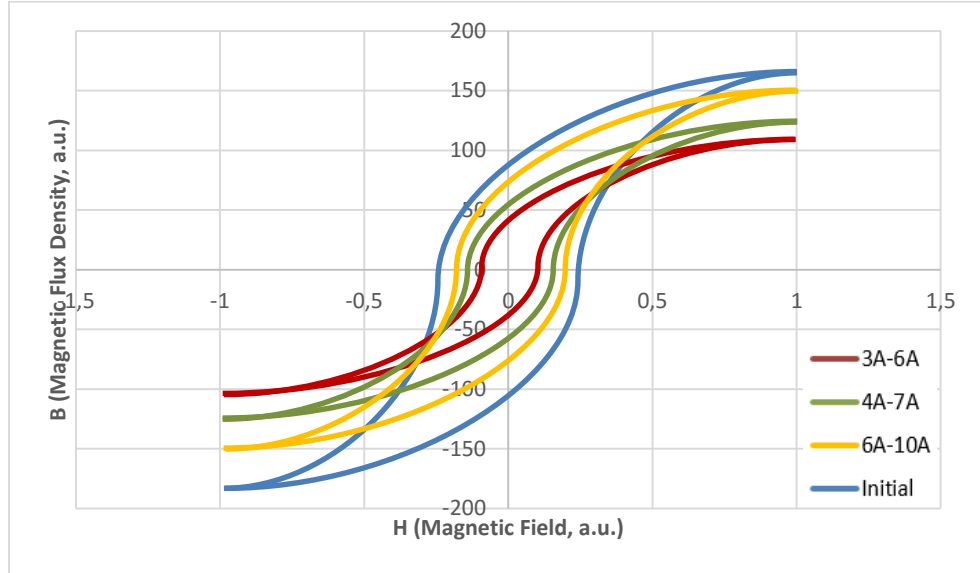


Figure 47 Representative hysteresis curves for different shot peening intensities

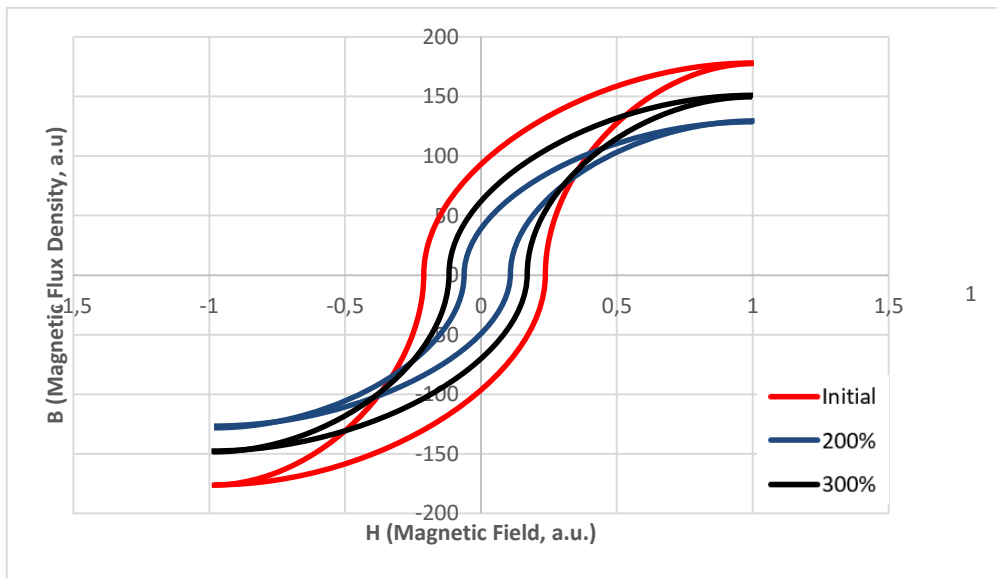


Figure 48 Representative hysteresis curves for different shot coverage values

MBN r.m.s. profiles were obtained by using μ scan channel of MBN equipment. Here, MBN profiles exhibited dissimilarity for shot peened and initial specimen due to formed compressive residual stress.

Table 5 MBN μ scan results

Sample Group #	Sample Code	Coverage (%)	Intensity	MBN RMS	MBN Peak	MBN Peak Position
G1	SP5	200	3A-6A	15.60	33.98	27.95
	SP19			15.48	33.08	28.59
	SP3			14.26	30.29	29.05
G2	SP17	300	3A-6A	14.78	31.77	28.36
	SP12			14.37	31.39	28.09
	SP20			17.36	38.82	28.23
G3	SP18	200	4A-7A	17.63	39.70	26.75
	SP14			16.41	37.65	27.15
	SP7			12.91	28.12	24.28
G4	SP1	300	4A-7A	15.80	34.28	26.44
	SP23			14.67	32.76	26.25
	SP11			19.65	45.72	26.36
G5	SP9	200	6A-10A	14.26	32.28	26.91
	SP15			18.28	40.80	27.05
	SP13			17.13	39.34	26.53
G6	SP10	300	6A-10A	19.45	44.63	26.98
	SP24			17.25	38.86	27.60
	SP21			15.19	34.06	27.29
Initial		Non-Shot Peened		19.08	43.00	28.01

MBN μ scan results were tabulated on *Table 5*. Accordingly, the sample having lowest Almen intensity shows lowest MBN RMS value. Similarly, lower coverage exhibits the lower MBN RMS values. Upon comparing MBN peak values, parallel outcome was signified with MBN RMS values. Peak positions of lower intensity exhibited higher magnetic field strength since having higher compressive residual stress made magnetization harder. To sum up, lower intensity and coverage parameters followed arrow direction exhibited in *Figure 49*. Ultimately, MBN profiles show parallel curves after saturation of peening process.

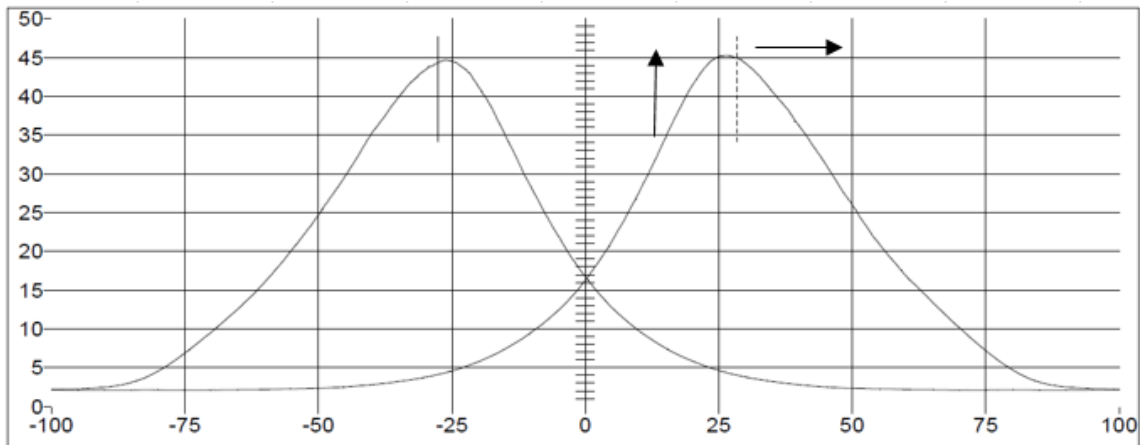


Figure 49 MBN profile versus magnetic field strength plot

5.3. RESULTS OF XRD MEASUREMENTS

Measurements through X-ray diffraction method were performed on the gage section of round specimen. The applied practice in this work consists of posing specimens at three different directions (0, 45, and 90). Each measurement includes the plots for 2theta-psi angle to peak intensity. The plot shows the occurrence of Bragg diffraction at different psi angles. XRD results were reported by ORS company.

Results were given with below *Table 6*. It should be noted that final measurement result is an approximation of averaged residual stress value. In addition to the axial direction, tangential stresses were also given in *Table 6* despite the fact that their effect in axial fatigue testing was not of primary importance.

Table 6 XRD measurement results

Sample Gr. #	Specimen Code	Shot Peening Parameter	Axial Residual Stress (MPa)	Tangential Residual Stress (MPa)
G1	SP5	3A-6A; %200	-50	-310
G6	SP10	6A-10A; %300	-60	-210

Average residual stress was measured approximately -70 MPa by MBN method for 3A-6A; %200 case. Same condition was measured axially -50 MPa by XRD. On the other hand, average residual stress was measured approximately -15 MPa by MBN method for 6A-10A; %200 case. Same condition was measured axially – 60 MPa by XRD. The root cause of discrepancy may be interpreted as uncertainty on XRD measurements. Residual stress measurements inherently incorporate uncertainty components stem from the following sources; elastic constants, instrument alignment, etc. Moreover, measurement depth was different for XRD (25 μm) and MBN (30-210 μm). Measurement volume is another parameter, accordingly spot size was 1 mm \varnothing for XRD; however, pickup area was 3 mm*1mm for MBN measurement.

Additionally, discrepancy may be caused by the grain size of the measured samples. XRD measurement is highly affected by the crystal texture and grain size. Samples having a large average grain size result in poor counting statistics and high amount of scatter. Hence number of diffracting grains in a unit area may not be enough to give a smooth intensity distribution in the peak.

Ideally, roughness value of the specimens shall be $R_a < 0.1$ for reliable XRD measurement. For higher roughness values, XRD method is usually not recommended and results incorporate intolerable uncertainty range. In the specimens the surface roughness was around 1.3 μm .

5.4. RESULTS OF FATIGUE TESTS

The first specimen in as-machined condition was tested under 400 MPa maximum load to decide suitable stress range for the rest of test matrix. The run-out criteria was chosen as $1.1\text{E}+07$ cycles. The specimen wasn't failed until $1.1\text{E}+07$ cycles and it was resulted as run-out and staircase method was applied. The test was continued in this sequence and maximum stress level was increased until 700 MPa with 100 MPa increments. In this point; the first specimen failed at $3\text{E}+05$ cycles. Required stress was determined as 700 MPa for the test matrix. In other words, rest of the specimens that contains different shot

peening parameters were tested under 700 MPa maximum stress and failed specimen results were tabulated in *Figure 50*.

All the specimens were executed with the same procedure in the case of being resistance of the specimens against applied stress particularly shot peened ones. Fatigue testing results are given in *Figure 50* and *Figure 51*.

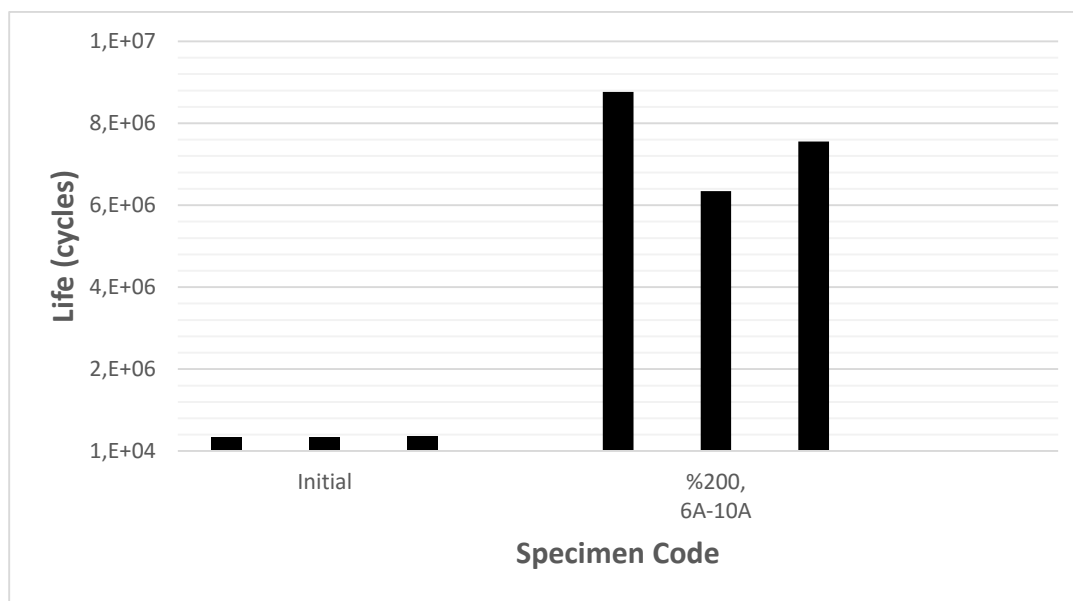


Figure 50 Fatigue test results for 700 MPa maximum stress (3 tests for each sample type)

The number of fatigue tests performed under each condition was three. The fatigue results are expressed as average values. Fatigue tests were considered finished after complete breakage of the specimen as %200, 6A-10A treatment or on reaching 1.0E+07 cycles (run-outs). The other specimens did not fail for 700 MPa maximum cyclic stress, thus their fatigue tests were interrupted according to the run-out criterion. For these samples, the block loading method was performed. According to the block loading method; increment step was determined as 50 MPa and new stress level was raised to 750 MPa. Eventually, their results are shown in *Figure 51*.

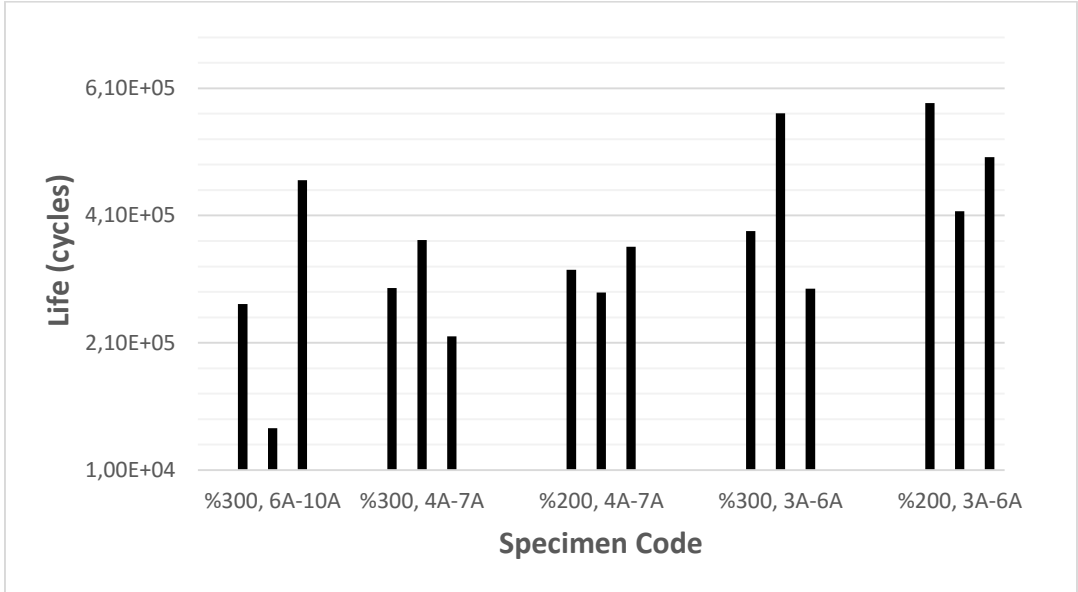


Figure 51 Fatigue test results for 750 MPa maximum stress (3 tests for each sample type)

Table 7 Fatigue test results for each parameter

Specimen Code	Max. Stress (MPa)	Average Cycles	St. Dev.
Initial	700	349.541	6.767
% 200, 6A-10A		7.564.419	1.208.663
% 300, 6A-10A		10.000.000	-
% 300, 4A-7A		10.000.000	-
% 200, 4A-7A		10.000.000	-
% 300, 3A-6A		10.000.000	-
% 200, 3A-6A		10.000.000	-
Initial		750	-
% 200, 6A-10A	-		-
% 300, 6A-10A	270.827		194.787
% 300, 4A-7A	295.978		75.631
% 200, 4A-7A	324.939		35.918
% 300, 3A-6A	417.204		140.534
% 200, 3A-6A	501.874		85.009

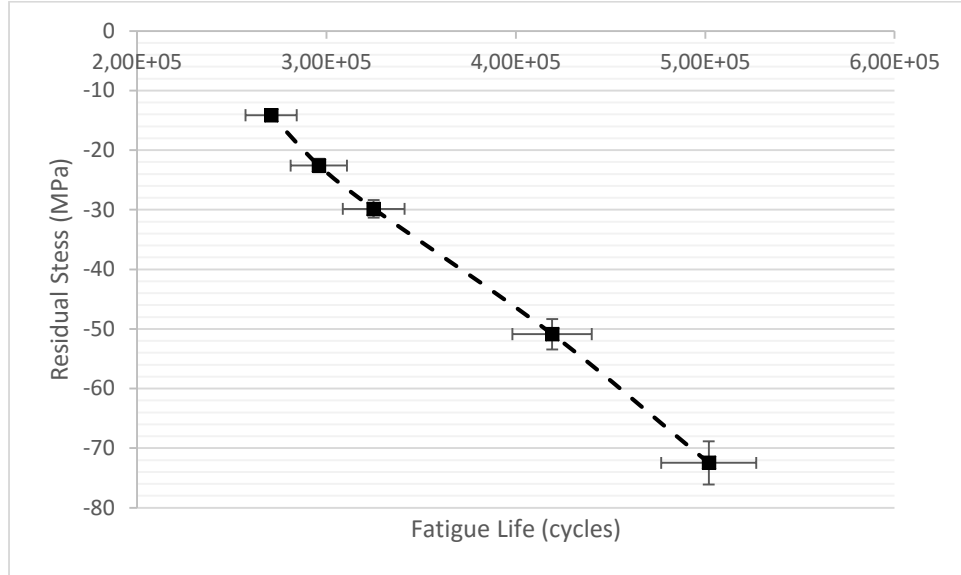


Figure 52 Effect of residual stress on fatigue life under maximum stress at 750 MPa
(MBN measurement)

All the shot peening treatments increased the fatigue life of the AISI 4140 steel compared to the non-treated specimens, the enhancement in fatigue life is increased with decreasing Almen intensity and coverage.



Figure 53 Representative fracture surfaces for each sample group

Relationship between compressive residual stress measured by MBN and fatigue life was exhibited on *Figure 52*. Accordingly, fatigue life of shot peened specimens was severely increased due to compressive residual stress on surface of samples that retarded crack formation period. Longer fatigue life resulted in larger crack propagation region explicitly. Additionally, fracture surfaces of failed samples were investigated by SEM. Cleavage and ductile regions of the failed specimen is shown on the *Figure 54*.

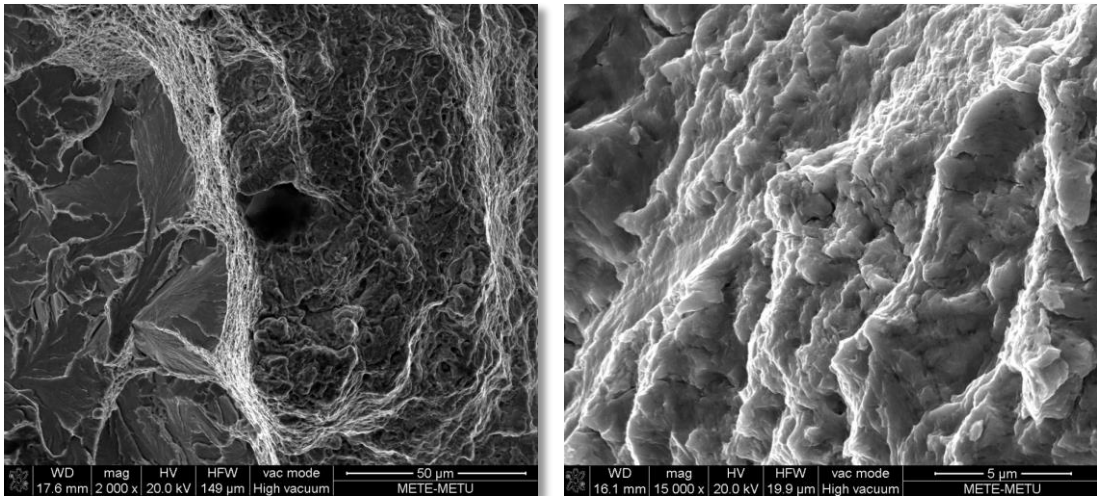


Figure 54 Representative SEM micrograph showing cleavage and ductile regions

Specimen-3 (3A-6A; %200) showing that higher fatigue life compared to specimen-24 (6A-10A; %300) had larger crack growth area as shown in *Figure 55*.



Figure 55 Fracture surfaces: SP3 [3A-6A %200] (left) & SP24 [6A-10A %300] (right)

To sum up; shot peening process is favorable for any type of materials without considering hard or soft in terms of advancement in fatigue life. In this study, 3A-6A intensity and %200 coverage parameters created highest residual stress value that was measured as 72 MPa. All in all, compressive residual stresses increased by decreasing Almen intensity and coverage for AISI 4140 steel. Diversity of the parameters makes the precise control difficult and very problematical therefore essential care shall be taken during shot-peening. The severity level was quantified by Almen strip to ensure the required intensity. Eventually, Almen strip measurements showed that desired shot-peening values were achieved. Residual stresses were measured in the skin depth range of 30-210 μm by MBN. After all, MBN method was successful technique for shot peened surfaces. Apart from that, signals for deeper regions can be achieved by operating at corresponding frequency for other applications. While MBN calibration, totally 12 measurements were performed by 30° intervals on the surface to find the specimen having least deviation and showing high reliability. The correct sensor contact shall be ensured by clips to secure the same contact pressure to each sample during MBN measurement. Surface roughness measurement was performed to eliminate the effect of machining problem causing premature failure during fatigue testing. MBN measurements were coherent with fatigue testing results that block loading was implemented to reveal endurance of material under cyclic loading. Ultimately, fatigue fracture surfaces were investigated by SEM in case of revealing suspicious test results.

CHAPTER 6

CONCLUSIONS

The aim of this study is to determine the surface residual stresses by the Magnetic Barkhausen Noise method (MBN), and by using this fast and practical non-destructive approach to estimate the fatigue life of the shot-peened AISI 4140 steels. Various samples were prepared by changing the shot-peening parameters, i.e., three Almen intensities (3-6, 4-7, 6-10 Almen) and two coverage values (200%, 300%). The samples were characterized by metallographic investigations and hardness measurements. After preparing the calibration curves between stress and the MBN signal peak values, MBN measurements were performed on the samples. The residual stress values estimated by the MBN method were compared with the results of XRD stress measurements, and acceptable correlations were obtained. Then, fatigue tests were performed at room temperature on the axial resonant testing machine, executing tensile-tensile cyclic loading with 140 Hz. Then, the correlations between the compressive residual stress and fatigue life, and also between MBN emission and fatigue life were established. The following conclusions can be drawn from this particular study:

- Compressive residual stresses created on the surface by shot peening improve the fatigue life of the AISI 4140 steel. Fatigue life increases with increasing magnitude of the surface compressive residual stress.
- The magnitude of the compressive residual stress is dependent upon the severity of shot peening, thus the parameters of the shot peening process.

- MBN emission is very sensitive to the changes in the residual stress state. It decreases with increasing magnitude of the compressive residual stress.
- By MBN measurements it is possible to control the success of the shot peening operations, and thus, to estimate the fatigue life of the components in a fast and practical way.

REFERENCES

- [1] Lundberg, M., Peng, R. L., Ahmad, M., Vuoristo, T., Bäckström, D., and Johansson, S. (2013). Influence of Shot Peening Parameters on Residual Stresses in Flake and Vermicular Cast Irons. *Materials Science Forum*, 768-769, 534-541.
- [2] Lopes, K. S., Sales, W. F., and Palma, E. S. (2008). Influence of machining parameters on fatigue endurance limit of AISI 4140 steel. *J. Braz. Soc. Mech. Sci. & Eng. Journal of the Brazilian Society of Mechanical Sciences and Engineering*, 30(1), 77-83.
- [3] Žerovnik, P., Fefer, D., and Grum, J. (2014). Surface Integrity Characterization Based on Time-Delay of the Magnetic Barkhausen Noise Voltage Signal. *Strojniški vestnik – Journal of Mechanical Engineering*, 60(1), 21-28.
- [4] Buttle, D. J. (2013). Magnetic Methods. *Practical Residual Stress Measurement Methods*, 225-258.
- [5] Boardman, B. Fatigue Resistance of Steels *ASM Handbook, Volume 1: Properties and Selection: Irons, Steels, and High-Performance Alloys*. ASM Handbook Committee, 673-688.
- [6] Eckersley, J. S. and Ferrelli B. (1993). Using shot peening to multiply the life of compressor components. *International Journal of Fatigue*, 15(6), 533.
- [7] Niku-Lari, A. (1987). Overview On The Shot Peening Process. *Advances in Surface Treatments*, 155-170.

- [8] Torres, M. (2002). An evaluation of shot peening, residual stress and stress relaxation on the fatigue life of AISI 4340 steel. *International Journal of Fatigue*, 24(8), 877-886.
- [9] Savas, S., and Gur, C. H. (2010). Monitoring variation of surface residual stresses in shot peened steel components by the magnetic Barkhausen noise method. *Insight - Non-Destructive Testing and Condition Monitoring*, 52(12), 672-677.
- [10] Palma, E., Mansur, T., Silva, S. F., and Alvarenga, A. (2005). Fatigue damage assessment in AISI 8620 steel using Barkhausen noise. *International Journal of Fatigue*, 27(6), 659-665.
- [11] Bhat, S., and Patibandla, R. (2011). *Metal Fatigue and Basic Theoretical Models: A Review, Alloy Steel - Properties and Use*, Dr. Eduardo Valencia Morales (Ed.), ISBN: 978-953-307-484-9.
- [12] Sutherland, H. J. (2000). A summary of the fatigue properties of wind turbine materials. *Wind Energy*, 3(1), 1-34.
- [13] Mitra, A., Govindaraju, M., and Jiles, D. (1995). Influence of microstructure on micromagnetic Barkhausen emissions in AISI 4140 steel. *IEEE Transactions on Magnetics*, 31(6), 4053-4055.
- [14] Stewart, D. M., Stevens, K. J. and Kaiser, A. B. (2004). Magnetic Barkhausen noise analysis of stress in steel *Curr. Appl. Phys* 4 308–11.
- [15] Pandey, R. K. and Deshmukh, M. N. (n.d.). Shot peening and its impact on fatigue life of engineering. *International Conference on Shot Peening and Blast Cleaning*. Retrieved March 16, 2017, on www.shotpeener.com/library/pdf/2001149.pdf
- [16] Hozapfel, H., Wick, A., and Vijhringer, O. (1996). Effect of Shot Peening Parameters on the Properties of Surface Layers in AISI4140 in Different Heat Treatment Conditions. *The Shot Peener*, Volume 10, Issue 1, 6-13.

- [17] N. A. Alang, N. A. Razak and A. K. Miskam (2011). Effect of Surface Roughness on Fatigue Life of Notched Carbon Steel, *International Journal of Engineering & Technology IJET-IJENS* Vol.: 11 No: 01.
- [18] Prévéry, Paul S. (1986). X-ray Diffraction Residual Stress Techniques, *Metals Handbook*. 10. Metals Park: American Society for Metals, 380-392.
- [19] Matzkanin, G. A. and Gardner, C. G. (1975). Measurement of Residual Stress Using Magnetic Barkhausen Noise Analysis. *Proceedings of the ARPA/AFML Review of Quantitative NDE*, June 1974–July 1975. Paper 27.
- [20] Image Source: on <http://www.people.vcu.edu/~jatulasimha/IntroToNanomagnetismGeneralAudience.html> (accessed on May 15, 2017)
- [21] Image Source: on <http://nptel.ac.in/courses/115103039/module1/lec1/5.html> (accessed on May 15, 2017)
- [22] Tönshoff, H.K., Friemuth, T., Oberbeck, I., Seegers, H. (2000). Micromagnetic Stress Determination on Tailored Blanks. , 15th WCNDT, 15-21 October 2000, Roma, S. 1-6.
- [23] Kurz, J., Szielasko, K., and Tschuncky, R. (2016). Micromagnetic and Ultrasound Methods to Determine and Monitor Stress of Steel Structures. *Journal of Infrastructure Systems*, 23(2), 1-9.
- [24] Image Source: on <https://www.manufacturingguide.com/en/shot-peening> (accessed on May 16, 2017)

- [25] Image Source: on <https://www.johndesmond.com/blog/metals/what-is-shot-peening/> (accessed on May 16, 2017)
- [26] Akyıldız, H. K., Kulekci, M. K., and Esme, U. (2015). Influence of shot peening parameters on high-cycle fatigue strength of steel produced by powder metallurgy process. *Fatigue & Fracture of Engineering Materials & Structures*, 38(10), 1246-1254.
- [27] Champaigne, J. M. (2006). Almen Gage Calibration. *Shot Peening*, 108-113.
- [28] Image Source: on <https://uwaterloo.ca/fatigue-stress-analysis-lab/research/residual-stress> (accessed on May 23, 2017)
- [29] Gujba, A., and Medraj, M. (2014). Laser Peening Process and Its Impact on Materials Properties in Comparison with Shot Peening and Ultrasonic Impact Peening. *Materials*, 7(12), 7925-7974.
- [30] Mohanty, S. K., and Arakerimath, R. R. (2016) ARB Life Improvement by Improvement in the Current Shot Peening Method. *International Journal for Research in Applied Science & Engineering Technology (IJRASET)*, Volume 4, Issue 1, 2321-9653.
- [31] Palacios, M., Bagherifard, S., Guagliano, M., and Pariente, I. F. (2014). Influence of severe shot peening on wear behavior of an aluminum alloy. *Fatigue & Fracture of Engineering Materials & Structures*, 37(7), 821-829.
- [32] González-Herrera, A., and Zapatero, J. (2005). Influence of minimum element size to determine crack closure stress by the finite element method. *Engineering Fracture Mechanics*, 72(3), 337-355.
- [33] Stráský, J., Havlíková, J., Bačáková, L., Harcuba, P., Mhaede, M., and Janeček, M. (2013). Characterization of electric discharge machining, subsequent etching and shot-

peening as a surface treatment for orthopedic implants. *Applied Surface Science*, 281, 73-78.

[34] Prevey, P. S. (1988). X-Ray Diffraction Testing Services at Lambda Research. *Jom*, 40(2), 54-55.

[35] Fitzpatrick, M. E. (2005). Determination of residual stresses by X-ray diffraction: issue 2. Teddington: National Physical Laboratory.

[36] Image Source: on <http://nessengr.com/home/technical-data/toroid-inductor-formulas-and-calculator/> (accessed on May 25, 2017)

[37] Standard practice for conducting force controlled constant amplitude axial fatigue tests of metallic materials. (2002). West Conshohocken, PA: ASTM.

[38] Deveci, M. (2016). Nondestructive determination of case depth by Barkhausen noise method. , Tampere University of Technology, Master's thesis. Retrieved from <https://dspace.cc.tut.fi/dpub/bitstream/handle/123456789/24049/deveci.pdf>

[39] Wang, P., Huang, K., Xu, J., Li, M., Zhang, Z., Tian, G., Psuj, G. (2015). Calculation of Magnetic Hysteresis Minor Loop and New Features Extraction based on Magnetic Barkhausen Noise. *Proceedings of the 2015 International Symposium on Material, Energy and Environment Engineering*.

[40] Monin, V., Teodosio R.J, Gurova, T., Assis, J.T. (2000). X-ray study of the inhomogeneity of surface residual stresses after shot-peening treatment. *Advances in X-ray Analysis*, 43, 48-53.

[41] Lammi, C.J. (2009). The effects of processing residual stresses on the fatigue crack growth behavior of structural materials. , Worcester Polytechnic Institute, Master's thesis. Retrieved from <https://web.wpi.edu/Pubs/ETD/Available/etd-120909132833/unrestricted/clammi.pdf>